

## Classification of inter-modular connections for stiffness and strength in sway corner-supported steel modular frames



M. Farajian<sup>a</sup>, P. Sharafi<sup>a,\*</sup>, H. Eslamnia<sup>b</sup>, K. Kildashti<sup>a</sup>, Y. Bai<sup>c</sup>

<sup>a</sup> Centre for Infrastructure Engineering, Western Sydney University, Penrith, Australia

<sup>b</sup> Department of Civil Engineering, Amirkabir University of Technology, Tehran, Iran

<sup>c</sup> Department of Civil Engineering, Monash University, Clayton 3800, Australia

### ARTICLE INFO

#### Keywords:

Modular frames  
Inter-modular connection  
Connection classification  
Rigid joints  
Stability analysis  
Effective length factor  
Sway frame  
Prefabricated prefabricated modular buildings  
Buckling capacity

### ABSTRACT

Corner-supported modular steel buildings, made of volumetric bespoke prefabricated units, are one of the most efficient construction systems for the next generation of prefabricated prefinished building construction. In these systems, the influence of connections between the units, so-called inter-connections, on the distribution of forces, moments, stability, and deformations of the frame is the key to the overall structural performance that differentiates the design of these systems from that of their conventional counterparts. In the design of modular buildings, the structural properties of inter-connections, such as stiffness, strength, and rotation capacity, are elements directly impacting their performance. This paper proposes a classification system for rotational stiffness and strength properties of inter-connections in sway corner-supported modular frames. The stiffness' boundary values corresponding to the rigid/semi-rigid and semi-rigid/nominally-pinned zones are represented by parametric charts based on the variation of relative bending stiffness ratios of elements such as beams, columns, and joints. To develop the classification system corresponding to stiffness properties of inter-connections, three performance criteria are assumed as (i) buckling criterion, which represents the classification based on the ultimate limit state; (ii) displacement/drift criterion, which considers the behaviour of the structure in the serviceability limit state; and (iii) combined buckling and displacement/drift criterion at the ultimate limit state. Furthermore, inter-connections are classified into three categories of fully-strength, partial-strength, and nominally-pinned in terms of their strength properties based on the ultimate moment capacity of inter-connections. The proposed classification system can be employed in the initial phase of a modular structure design to classify joints, and select a proper design method and process according to their category. Numerical examples are included to verify the validity of the proposed classification system. Finally, design recommendations are suggested for the accurate design of inter-connections in sway corner-supported modular frames without the need for complicated nonlinear analyses.

### 1. Introduction

Volumetric modular construction refers to a manufacturing based construction concept, in which three dimensional modules are prefabricated in the factory and assembled on-site through the use of the so-called inter-modular connections or inter-connections to form a permanent structure. Construction of high-rise modular buildings is a relatively contemporary yet fast-growing technology, which has inadequate pilot buildings as benchmarks to accomplish some specifications in terms of loading transfer mechanisms and interactions between units. On the other hand, due to the discrete nature of modular buildings,

massive connections for different structures are required, while the complexity of connections and interactions between elements and units remains a key issue. The ever-increasing use of new and innovative modular connections in the construction of multi-storey buildings compounds these difficulties [1,2]. The role of horizontal and vertical inter-connections is vital for providing structural stability and integrity, especially when it comes to high-rise modular buildings [3–5]. The lack of continuity in the joints, due to the presence of inter-connections in addition to the beam-to-column connections, so-called intra-connections, made the static and dynamic characteristics of these structures unforeseeable, when they are subjected to different types of loading [6].

\* Corresponding author.

E-mail address: [sharafi@westernsydney.edu.au](mailto:sharafi@westernsydney.edu.au) (P. Sharafi).

**Fig. 1** shows the detail of a general joint in the perimeter frame of a sway corner-supported modular frame, in which the horizontal and vertical connectivity is provided by the end plate connections. Up to four columns and eight beams can intersect in a single joint in perimeter frame of a corner-supported systems.

While most traditional building codes and standards are not particularly pertinent to the design of modular buildings, considerations should be given to the distinctive components and processes of modular structures, such as the design of inter-connections. The lack of sufficient research on the performance of inter-connections results in the design of modular frames based on the available standards and codes for conventional structures, regardless of the fact that they may have different behaviour and performance [7,8]. Many inter-connections are categorized as connections with semi-rigid behaviour based on the available classification for beam-to-column connections [9,10]. The consequences of such an assumption in the design of modular frames is a need for accurate modelling and analysing of a structure, which is a time-consuming procedure, resource-intensive and costly. Furthermore, the engineers may have to take risks due to the uncertainty and dissimilarity of the behaviour of such complex joints [1]. Within this context, a classification system enhancing the reliability and predictability of inter-connections behaviour can play an essential role in facilitating the design of these systems.

Generally, joints in structures are categorized based on their mechanical properties, including stiffness, strength, and ductility. Eurocode 3 part 1.8 [11] suggests various behaviour of joints based on the method of global analysis of structures. For the elastic analysis, it recognises three classes of joints as nominally pinned, rigid and semi-rigid. The stiffness of semi-rigid connections has to be taken into consideration in the design process. The choice of joint's model may significantly influence deformations, distribution of internal forces, and load-carrying capacity of elements in a system. The objective of a classification system is to define accurate boundaries for behavioural classes of joints and to establish useful criteria allowing for a safe use of continuous or simple modelling of joints [12]. While extensive research is performed on the stiffness of beam to column connections and its influence on structural performance (e.g. [13–16]), the literature is silent on the joint classification in corner-supported modular frames.

Proposals for the classification of connections are suggested by Eurocode 3 [11] and Bjorhovde et al. [17]. The classification system proposed by Eurocode 3 is more appropriate when the layout and member details of the structure are identified in advance. On the other hand, the classification system developed by Bjorhovde et al. is based on the reference length of beam elements, and it is more suitable when the frame layout, configurations, and members details are not available. The precise boundary values corresponding to rigid/semi-rigid zones as well as semi-rigid/pinned zones are presented by Eurocode 3 and Bjorhovde et al.

[11,17]. The behaviour of different beam-to-column connections is studied by Kishi and Chen [18], which is used for the evaluation of rigidity of the extended end plate connections by Hasan et al. [19]. Hasan et al. [20] developed a classification system considering the nonlinear behaviour of connections. The validity of the classification system proposed by Eurocode 3 and Bjorhovde et al. is examined through the elastic-plastic finite displacement analysis [21]. Goto et al. [22] established a classification system for connections and determined the boundary value of rigid/semi-rigid zones considering the serviceability and ultimate limit states simultaneously. Gomes et al. [23] suggested a classification system for joints in reinforced concrete structures by taking into consideration the shear deformation component of joints. The unique classification system developed by Nethercot et al. [24] considers the stiffness and strength properties of a connection at the same time. They categorized the connections into four groups: fully-connected, partially-connected, pinned-connected, and non-structural. Fan et al. [25] established a connection classification for joints in lattice shells where the joints are categorized based on their stiffness and strength. Wang and Chen developed a classification system for tabular joints in lattice girders and studied the influence of joint characteristics on responses of lattice girders [26].

This paper, which is a part of a broad project on the compliance criteria for the design of inter-connections, being in progress in Western Sydney University, develops a classification system for the rotational component of horizontal and vertical inter-connections, and evaluates their effects on responses of sway corner-supported modular frames. The proposed classification for inter-connections can significantly simplify the design and analysis procedures of modular structures. Besides, it facilitates the incorporation of new additional connection types into categories, once tests and other descriptive data are available. The developed classification system categorizes the inter-connections based on their stiffness and strength. In the section two, the performance criteria, required for the classification of connections based on the stiffness and strength are described. Three performance criteria are considered for the stiffness classification of inter-connections (i) buckling criterion, in which the governing equations of buckling of columns are derived for the classification in the ultimate limit state, (ii) displacement/drift criterion, in which parametric modelling is performed for the classification in the serviceability limit state, and (iii) combined buckling and displacement/drift criterion at the ultimate limit state. In the third section, the methodology, which is followed, to determine the boundary values for the development of classification system are explained. The fourth section deals with the modelling procedures for establishing classification systems. In the chapter five the classification system is developed. For the buckling and drift criteria, the classification system is provided in the form of three-dimensional contour charts for various relative bending stiffness ratios of joint elements such as beams, columns, and connections. The section six verifies the

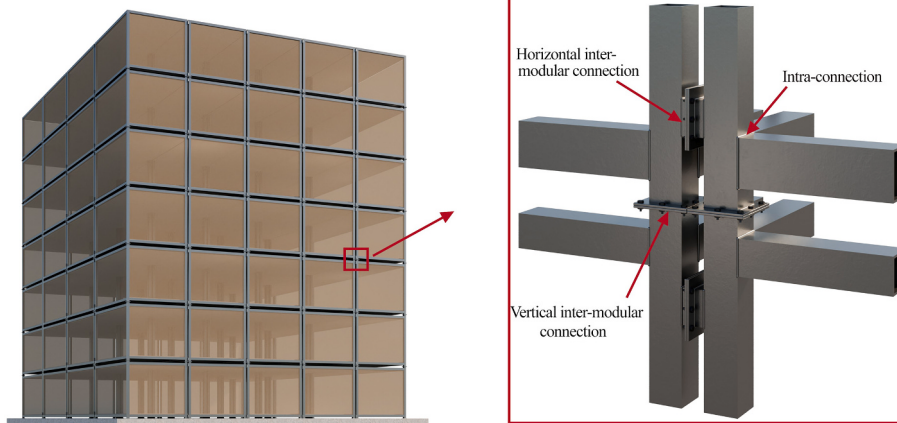


**Fig. 1.** A typical joint in a perimeter frame of sway corner-supported modular building.

established classification system through a case study. Moreover, for the combined buckling and displacement at the ultimate limit state, the classification is performed for a case study sway modular frame. In addition, the boundary values for the strength properties of inter-connections are suggested, enabling them to be classified as full-strength, partial-strength, and nominally-pinned. Finally, some recommendations for the design and analysis of inter-connections are suggested in the section 7.

## 2. Performance criteria for the classification of inter-connections in sway frames

One of the most popular and well-accepted classification systems is the one proposed by Eurocode 3, in which the classification systems are suggested separately for non-sway and sway frames. Eurocode 3 arranges connections based on their strength and stiffness. In terms of strength properties, it puts the labels of full-strength, partial-strength, and nominally pinned on connections by comparing the ultimate moment capacity of connections ( $M_u$ ) with the design plastic moment of connection's adjacent elements [11]. On the other hand, for stiffness characteristics, connections are classified as rigid, semi-rigid, and nominally pinned. The boundary between rigid and semi-rigid zones is determined such that the load-carrying capacity of a column in a portal frame with semi-rigid connections ( $P_{cr,SR}$ ) does not drop more than 5% of the corresponding rigid frame ( $P_{cr,R}$ ) [11,27]. In a similar fashion, the boundary between semi-rigid and nominally-pinned zones is determined such that the load-carrying capacity of a column in a portal frame with pinned behaviour ( $P_{cr,P}$ ) does not drop more than 75% of that of the portal frame with rigid connections [24]. The load-carrying capacity, or buckling capacity, of a column can be obtained through the Euler formula, expressed as:

$$P_{cr} = \frac{\pi^2 EI}{(KL)^2} \quad (1)$$

where  $E$ ,  $I$ ,  $L$ , and  $K$  are modulus of elasticity, moment of inertia, length, and effective length factor of column element, respectively. It is shown that the  $K$  factor of column and therefore its buckling capacity, can be changed through the variation of end columns' stiffness [16,22,25,27,28]. In fact, according to the slope-deflection method the governing buckling equations of a column varies based on the rotational stiffness of elements connected to the column. Therefore, in this paper the effective length factor of column which representing the buckling capacity of a column is considered to establish the classification charts. However, the behaviour of structure in the serviceability limit state is not considered by Eurocode 3 [22]. Therefore, Eq. (3) which take into

account the drift of the structure at the serviceability limit state is added as a new criterion (Eqs. (3) and (6)) [22,24]. Moreover, Goto et al. [22] stated that the Eq. (2) may not be sufficient because the displacement at the ultimate limit state is not reflected. To tackle this issue, they proposed to investigate the behaviour of structures by considering the buckling capacity and displacement at the ultimate limit state through their square root of sum of the squares (Eq. (4)) [22].

In this study, the effective length factor ( $K$ -factor) of columns and drift of structures, which represent the behaviour of structures at the ultimate and serviceability limit states, are considered for the classification of inter-connections based on the stiffness properties. Furthermore, the classification based on the buckling capacity and drift at the ultimate limit state is conducted. Pursuing Eurocode 3, the criteria to define the boundaries of various zones based on both strength and stiffness are listed in Table 1.

## 3. Methodology

A methodology is required to facilitate the establishment of a classification system for rotational stiffness of inter-connections. Fig. 2 indicate the flowchart of the methodology used in this study to develop the classification charts.

According to the methodology used in this paper, at the first step, a large value is assigned to the rotational stiffness of inter-connections. This results in to obtain the response of the structure when the inter-connections have a rigid behaviour. At the second step, a small value is assigned to the rotational stiffness of inter-connections, leading to determine the response of the structure when the inter-connections have a pinned behaviour. Having the response of the structure in these two extreme conditions, it can be decided whether a classification is required or not; that is if the difference between these two extreme conditions is less than 5%, the behaviour of inter-connection has no effect on the response of the system. On the other hand, if the difference is more than 5%, then, the stiffnesses corresponding to 5% drop in the response of the system with rigid behaviour can be determined as the boundary values of rigid/semi-rigid zone through the trial-and-error procedure. Similarly, in order to determine the boundary values corresponding to semi-rigid/pinned zones, a trial-and-error procedure is followed to determine the 75% reduction in the response of the structure corresponding to rigid behaviour of inter-connections.

## 4. Modelling inter-connections for the classification of stiffness in sway modular frames

A general assemblage of a sway modular frame consisting of several

**Table 1**

Criteria for the classification of inter-connections.

Characteristics				
Strength	Stiffness			
Boundary	Criteria	Boundary	Limit state	Criteria
Full-strength /partial strength	$M_u = M_{pc}$	Rigid/semi-rigid	Ultimate	$\left  \left( \frac{P_{cr,R} - P_{cr,SR}}{P_{cr,R}} \right) \right  = 0.05 \quad (2)$
			Serviceability	$\left  \left( \frac{\Delta_R - \Delta_{SR}}{\Delta_R} \right) \right  = 0.05 \quad (3)$
			Combined ultimate and serviceability	$\sqrt{\left( \frac{P_{cr,R} - P_{cr,SR}}{P_{cr,R}} \right)^2 + \left( \frac{\Delta_{uR} - \Delta_{uSR}}{\Delta_{uR}} \right)^2} = 0.07 \quad (4)$
Partial-strength / nominally pinned	$M_u = 0.25M_{pc}$	Semi-rigid/nominally pinned	Ultimate	$\left  \left( \frac{P_{cr,R} - P_{cr,P}}{P_{cr,R}} \right) \right  = 0.75 \quad (5)$
			Serviceability	$\left  \left( \frac{\Delta_R - \Delta_P}{\Delta_R} \right) \right  = 0.75 \quad (6)$

- $P_{cr,R}$ ,  $P_{cr,SR}$  and  $P_{cr,P}$  are buckling capacity of a column corresponding to rigid, semi-rigid and pinned inter-connections.
- $\Delta_R$ ,  $\Delta_{SR}$  and  $\Delta_P$  are the drift of a structure corresponding to rigid, semi-rigid and pinned inter-connections.
- $\Delta_{uR}$  and  $\Delta_{uSR}$  are the displacement/drift of a structure with rigid and semi-rigid behaviour of inter-connections at the ultimate limit state.
- $M_u$  and  $M_{pc}$  are the ultimate moment of connection and plastic moment of its adjacent column.

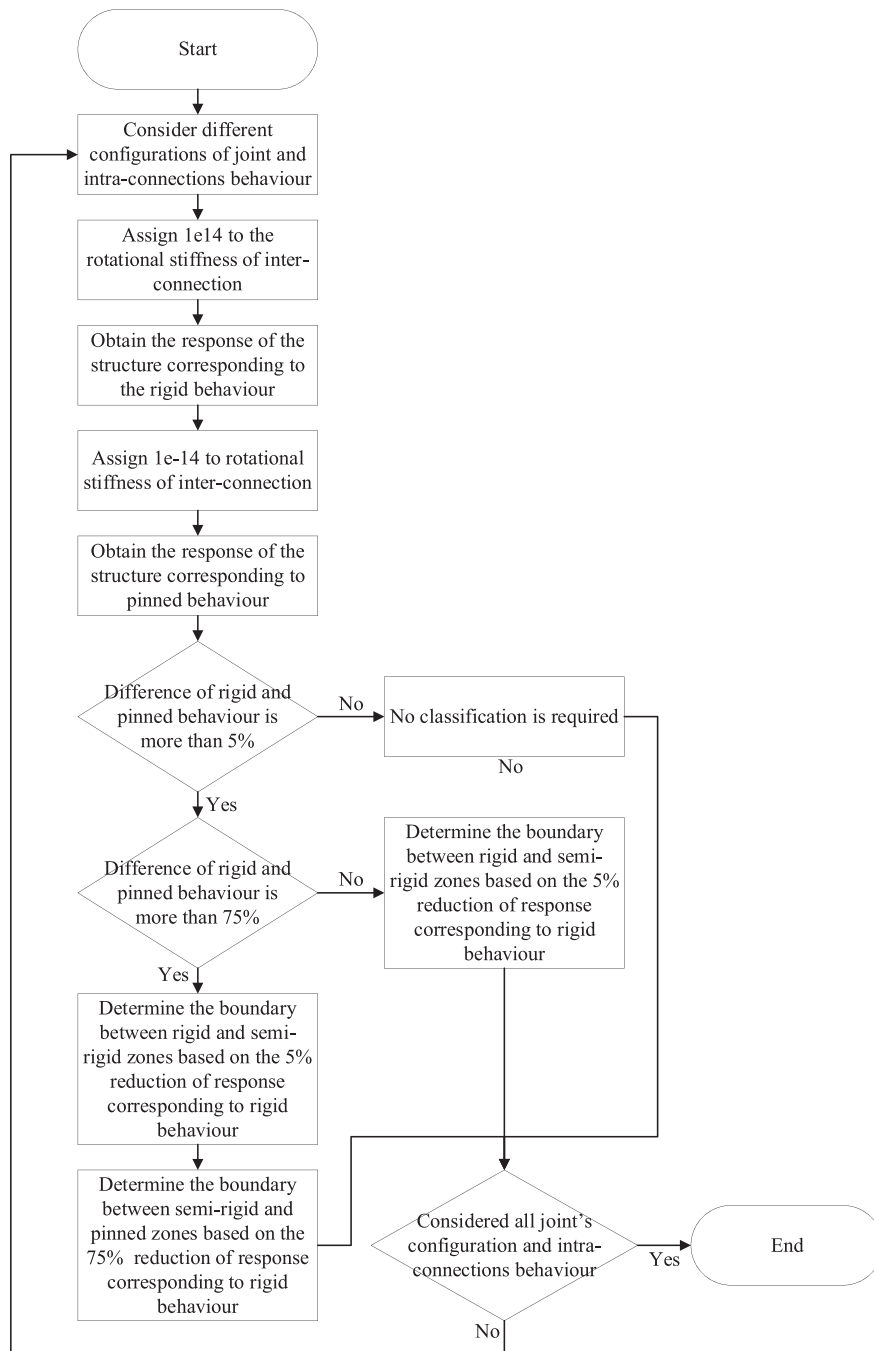


**Fig. 2.** Flowchart of the methodology used in this paper.

modules being connected by horizontal and vertical inter-connections is shown in Fig. 3, in which intra-connections are demonstrated by rotational springs, and inter-connections are illustrated by springs having axial, shear, and rotational stiffness. These connections are shown by a simple line in the figure for the simplicity. However, as it is shown, each inter-connections have three degree-of-freedom, providing the ability to have vertical, horizontal and rotational deformation. For the horizontal inter-connection, the axial component of inter-connection (in X direction) provides the ability for horizontal deformation. On the other hand, the shear component of horizontal inter-connection (in Z direction) can provide the connection to have a vertical deformation. Finally, the bending component provide the rotation of the structure in horizontal direction about Y direction. Regarding the vertical inter-connection, while the axial component of provides the ability to deform in the Z

direction, its shear component provides the capability in the X direction. Finally, the bending component of vertical inter-connection provide the ability for the structure to rotate about the Y direction and displacement in X direction.

#### 4.1. Governing equations for buckling analysis of columns in sway modular frames

The effective length factor of columns ( $K$ -factor) in sway corner-supported steel modular structures is studied by Farajian et al. [6], where they derived the governing equations for elastic buckling load of columns, considering the stiffness of inter-connections, to investigate the effective length factor of a column in horizontally- and vertically-connected sway modular frames. A more general form of buckling

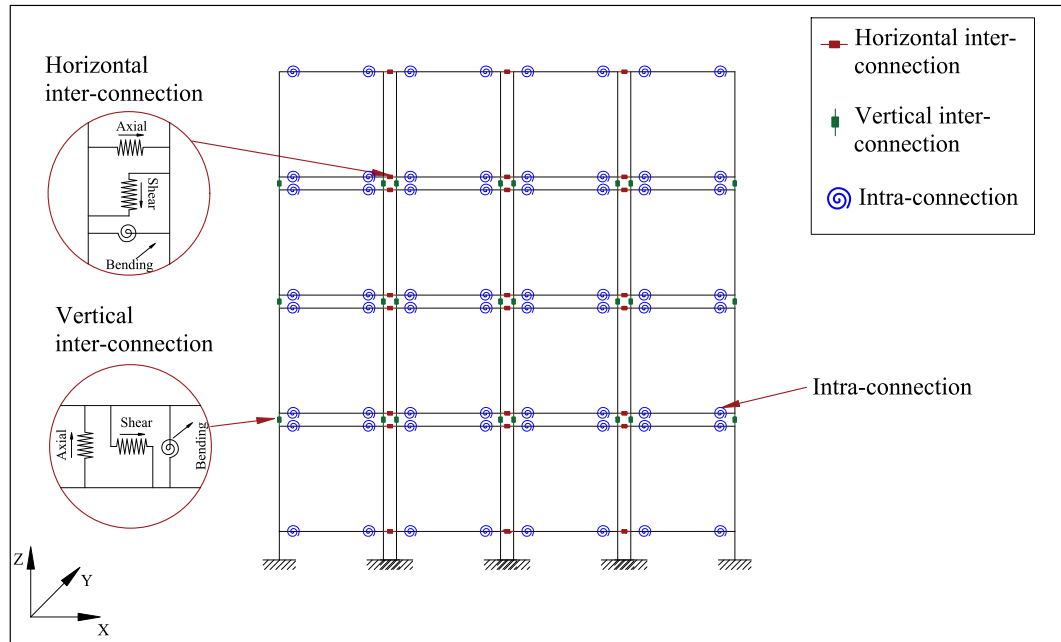


Fig. 3. A general assemblage model of a sway corner-supported modular frame.

equations, derived in [6], is presented here, in order to take into account the flexibility of intra-connections; that is while the previous study includes only the rigid behaviour of intra-connections, in this study a wide range of behaviours consisting rigid and semi-rigid behaviour is considered for the intra-connections through incorporation of a flexibility factor in the governing buckling equations. Fig. 4 shows a general assemblage model of a sway modular frame consisting of six corner-supported modules with their inter- and intra-connections. The horizontal and vertical inter-connections, shown in Fig. 4, connect column  $c_4$  in the general assemblage to the adjacent elements (five columns and eight beams). The general assemblage of the corner-supported modular structure can be split into two sub-assemblages; hence, the classification system is established corresponding to horizontal and vertical inter-connections. This provides structural designers to accurately considered the behaviour of each type of inter-connections. The two sub-

assemblages are shown in Fig. 5 (a) and Fig. 5 (b), respectively.

The first sub-assemblage (Fig. 5 (a)) includes two horizontal modules that are connected by two horizontal inter-connections ( $S_{h1}$  and  $S_{h2}$ ). On the other hand, the second sub-assemblage, shown in Fig. 5 (b), is composed of three vertically stacked modules connected by vertical inter-connections. The undeformed and deformed shapes of the beam element  $AB$  are depicted in Fig. 5 (c). The end moment in this element ( $M_{AB}$ ) is the same as that in conventional structures, which depends on the modulus of elasticity ( $E$ ), the moment of inertia ( $I_b$ ), and the length of the beam ( $L_b$ ) as well as the rotation at end A ( $\theta_A$ ). The deformed and undeformed shapes of the beam-column element  $CD$  are depicted in Fig. 5 (d). The end moments in a beam-column element subjected to an axial force  $P$  are the same as that of conventional structures. The end moments of beam-column element  $CD$  ( $M_{CD}$  and  $M_{DC}$ ) are functions of the stability functions ( $s_{ii}$  and  $s_{ij}$ ), length of the beam-column element

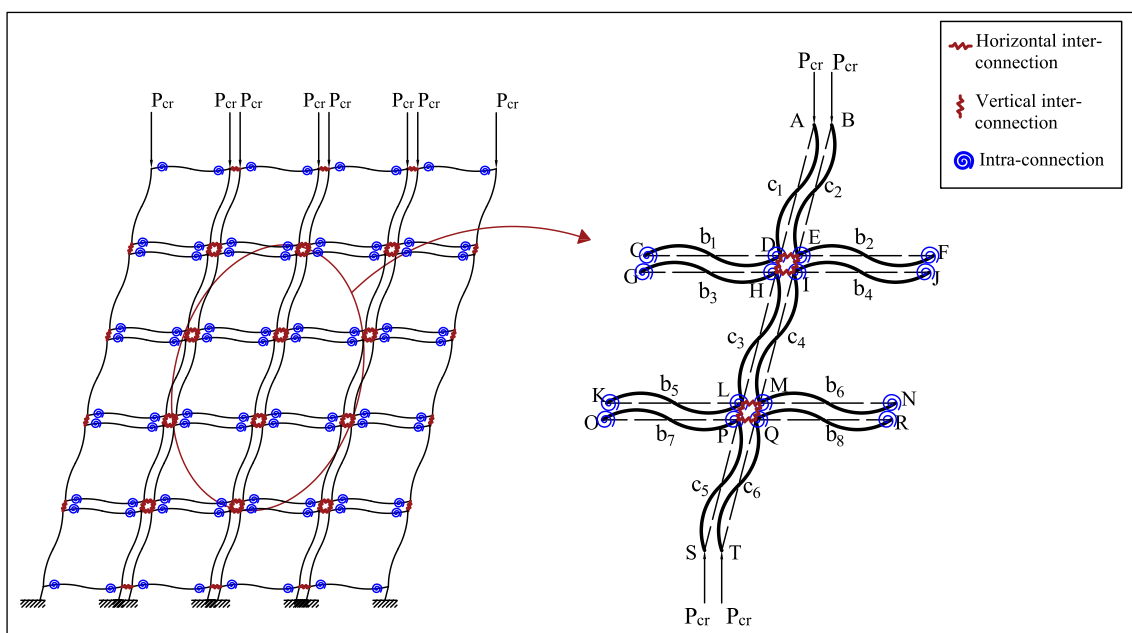


Fig. 4. A general assemblage model for buckling analysis of a sway modular frame.

( $L_c$ ), the moment of inertia of beam-column element ( $I_c$ ), and rotations at the end C and D ( $\theta_C$  and  $\theta_D$ ), respectively. The moment equations for beam and beam-column elements ( $M_{AB}$ ,  $M_{CD}$ , and  $M_{DC}$ ) of sway modular frames are stated in detail in [6].

#### 4.1.1. Governing buckling equations for columns in horizontally connected sway modular frames

Fig. 5 (a) illustrates the sub-assemblage model to derive governing buckling equations for a column in a horizontally connected sway modular frame. It is composed of column  $c_4$ , which is restrained by two horizontal inter-connections ( $S_{h1}$  and  $S_{h2}$ ), column  $c_3$ , beams  $b_3$ ,  $b_4$ ,  $b_5$ , and  $b_6$ , respectively. Using the slope-deflection method, the general equilibrium and compatibility equations lead to Eqs. (6) and (7), respectively. The detail of the slope-deflection method to derive the governing equations of buckling is found in the study conducted by

$$C = \frac{i_{c4}}{i_{c3}} \quad (11)$$

where,  $i_{bn}$  and  $i_{cn}$  are the bending stiffness of beam and column of element  $n$  ( $EI_b/L_b$  and  $EI_c/L_c$ ), and  $R_{Shi}$  is the rotational stiffness of horizontal inter-connection at node  $i$ . Because, in reality, one type of inter-connections with the same rigidity is employed, the stiffness of horizontal inter-connections is illustrated by  $R_{Sh}$ . The  $\alpha_{bf}$  is a coefficient representing the flexibility/rigidity of intra-connections depending on the rigidity of intra-connection at ends A and B of the beam element as listed in Table 2 [29].

The rotational stiffness of intra-connections at nodes A and B of the beam element, shown in Fig. 5 (c), are represented by  $R_{kA}$  and  $R_{kB}$ , respectively. Since, in practice, one type of intra-connections is used in a structure, the rotational stiffness of intra-connections at the ends of

$$\begin{aligned} & \left[ (6CG'_I + 6G'_H + Cs_{ii} + s_{ii}) \prod_{k=I,M} SR_{kH} + SR_{MH} \left( 36 \prod_{k=H,J} G'_k + 6s_{ii} \sum_{k=H,J} G'_k + s_{ii}^2 \right) - SR_{IH} s_{ij}^2 \right] \theta_I + \\ & \left[ s_{ij}(C+1) \prod_{k=I,M} SR_{kH} + SR_{MH} s_{ij} (6G'_H + s_{ii}) - SR_{IH} s_{ij} (6G'_M + s_{ii}) \right] \theta_M - \left[ (Cs_{ii} + Cs_{ij} + s_{ii} + s_{ij}) \right. \\ & \left. \prod_{k=I,M} SR_{kH} + SR_{MH} \left( 6G'_H \sum_{k=i,j} s_{ik} + s_{ii}^2 \right) - s_{ij}^2 SR_{IH} + s_{ii}s_{ij}(SR_{MH} - SR_{IH}) \right] \frac{\Delta}{L_c} = 0 \quad (7) \\ & \left[ s_{ij}(C+1) \prod_{k=I,M} SR_{kH} + SR_{MH} s_{ij} (6G'_I + s_{ii}) - SR_{IH} s_{ij} (6G'_L + s_{ii}) \right] \theta_I + \left[ \left( 6CG'_M + 6G'_L + Cs_{ii} + \right. \right. \\ & \left. \left. s_{ii} + s_{ij} \right) \prod_{k=I,M} SR_{kH} - SR_{IH} \left( 36 \prod_{k=M,L} G'_k + 6s_{ii} \sum_{k=L,M} G'_k + s_{ii}^2 \right) + SR_{MH} s_{ij}^2 \right] \theta_M - \left[ \left( Cs_{ii} + Cs_{ij} + \right. \right. \\ & \left. \left. s_{ii} + s_{ij} \right) \prod_{k=I,M} SR_{kH} - SR_{IH} \left( 6G'_L \sum_{k=i,j} s_{ik} + s_{ii}^2 \right) + SR_{MH} s_{ij}^2 + s_{ii}s_{ij}(SR_{MH} - SR_{IH}) \right] \frac{\Delta}{L_c} = 0 \quad (8) \end{aligned}$$

Farajian et al. [6].

in which,  $G'$ ,  $SR_{ih}$ , and  $C$  are the relative bending stiffness ratio of beams to columns, the relative bending stiffness ratio of horizontal inter-connections to columns at node  $i$ , and the bending stiffness ratio of column  $c_4$  to that of column  $c_3$ , obtained through the Eqs. (8) to (10), respectively; and  $i$  denotes the node name, i.e.  $I$ ,  $H$ ,  $M$ , and  $L$ . The parameter ( $\Delta/L_c$ ) is obtained from the shear equation of the sub-assemblage [6].

$$G'_I = \frac{\alpha_{bf} i_{b4}}{i_{c4}}, \quad G'_H = \frac{\alpha_{bf} i_{b3}}{i_{c3}}, \quad G'_M = \frac{\alpha_{bf} i_{b6}}{i_{c4}}, \quad G'_L = \frac{\alpha_{bf} i_{b5}}{i_{c3}} \quad (9)$$

$$SR_{IH} = \frac{R_{Sh1}}{i_{c4}}, \quad SR_{MH} = \frac{R_{Sh2}}{i_{c3}} \quad (10)$$

beams is equal in value. As a result, the stiffness of intra-connections is shown by  $R$  in this study. For the parametric study and incorporate the stiffness of intra-connections, the relative bending stiffness ratio of beam-to-column connections is defined as:

$$\rho = \frac{EI_b}{L_b R} \quad (12)$$

Eqs. (6) and (7) are rewritten in a matrix form as:

$$\begin{bmatrix} \beta_1 & \beta_2 \\ \beta_3 & \beta_4 \end{bmatrix} \begin{Bmatrix} \theta_I \\ \theta_M \end{Bmatrix} = 0 \quad (13)$$

The coefficients  $\beta_1$ ,  $\beta_2$ ,  $\beta_3$ , and  $\beta_4$  are coefficients expressed by Eqs. (14) to (17).

$$\begin{aligned} \beta_1 = & (6CG'_I + 6G'_H + Cs_{ii} + s_{ii}) \prod_{k=I,M} SR_{kH} + SR_{MH} \left( 36 \prod_{k=H,J} G'_k + 6s_{ii} \sum_{k=H,J} G'_k + s_{ii}^2 \right) - SR_{IH} s_{ij}^2 \\ & - \frac{(s_{ii} + s_{ij})}{2(s_{ii} + s_{ij})^2} \left[ (Cs_{ii} + Cs_{ij} + s_{ii} + s_{ij}) \prod_{k=I,M} SR_{kH} + SR_{MH} \left( 6G'_H \sum_{k=i,j} s_{ik} + s_{ii}^2 \right) - s_{ij}^2 SR_{IH} + \right. \\ & \left. s_{ii}s_{ij}(SR_{MH} - SR_{IH}) \right] \end{aligned} \quad (14)$$

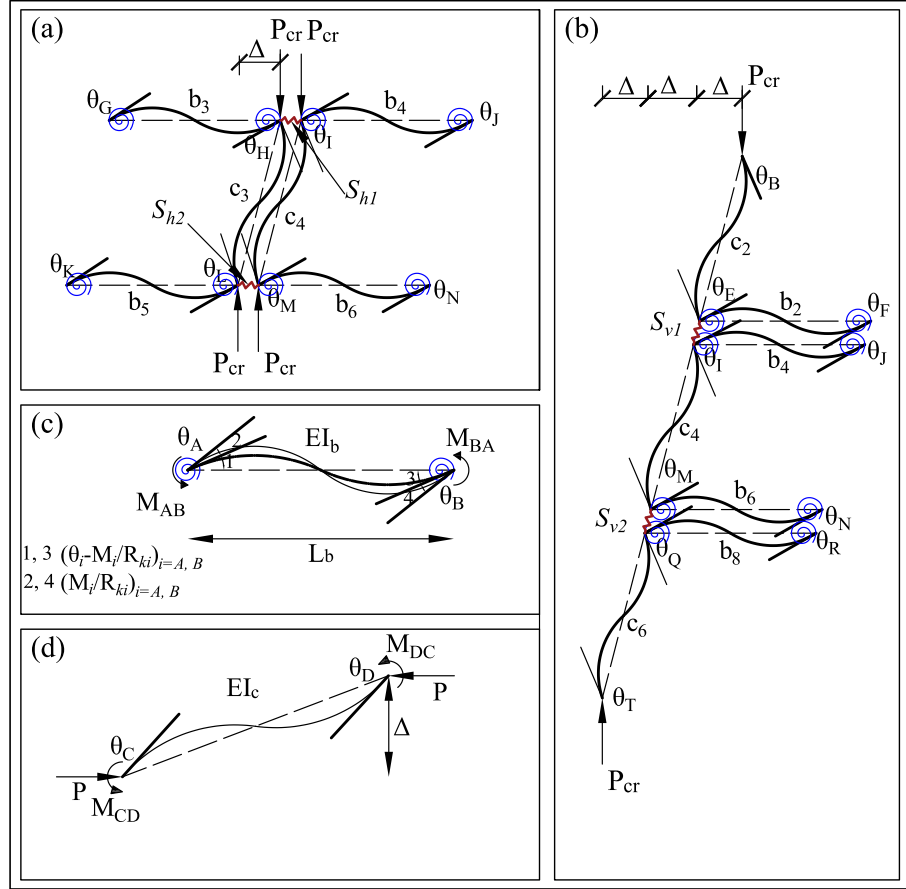


**Fig. 5.** (a) sub-assemblage model for horizontal inter-connections in a sway frame; (b) sub-assemblage model for vertical inter-connections in a sway frame (c) beam element in a sway frame subjected to end moments (d) beam-column element in a sway frame subjected to axial load and end moments.

$$\beta_2 = s_{ij}(C+1) \prod_{k=I,M} SR_{kh} + SR_{MH}s_{ij}(6G'_H + s_{ii}) - SR_{IH}s_{ij}(6G'_M + s_{ii}) - \frac{(s_{ii} + s_{ij})}{2(s_{ii} + s_{ij}) - (kL_C)^2} \\ \left[ (Cs_{ii} + Cs_{ij} + s_{ii} + s_{ij}) \prod_{k=I,M} SR_{kh} + SR_{MH} \left( 6G'_H \sum_{k=i,j} s_{ik} + s_{ii}^2 \right) - s_{ij}^2 SR_{IH} + s_{ii}s_{ij}(SR_{MH} - SR_{IH}) \right] \quad (15)$$

$$\beta_3 = s_{ij}(C+1) \prod_{k=I,M} SR_{kh} + SR_{MH}s_{ij}(6G'_I + s_{ii}) - SR_{IH}s_{ij}(6G'_L + s_{ii}) - \frac{(s_{ii} + s_{ij})}{2(s_{ii} + s_{ij}) - (kL_C)^2} \\ \left[ (Cs_{ii} + Cs_{ij} + s_{ii} + s_{ij}) \prod_{k=I,M} SR_{kh} - SR_{IH} \left( 6G'_L \sum_{k=i,j} s_{ik} + s_{ii}^2 \right) + SR_{MH}s_{ij}^2 + s_{ii}s_{ij}(SR_{MH} - SR_{IH}) \right] \quad (16)$$

$$\beta_4 = (6CG'_M + 6G'_L + Cs_{ii} + s_{ii}) \prod_{k=I,M} SR_{kh} - SR_{IH} \left( 36 \prod_{k=M,L} G'_k + 6s_{ii} \sum_{k=L,M} G'_k + s_{ii}^2 \right) + SR_{MH}s_{ij}^2 \\ - \frac{(s_{ii} + s_{ij})}{2(s_{ii} + s_{ij}) - (kL_C)^2} \left[ (Cs_{ii} + Cs_{ij} + s_{ii} + s_{ij}) \prod_{k=I,M} SR_{kh} - SR_{IH} \left( 6G'_L \sum_{k=i,j} s_{ik} + s_{ii}^2 \right) + SR_{MH}s_{ij}^2 + s_{ii}s_{ij}(SR_{MH} - SR_{IH}) \right] \quad (17)$$

The effective length factor ( $K$ -factor) of column  $c_4$  is then obtained through Eq. (18).

$$\begin{vmatrix} \beta_1 & \beta_2 \\ \beta_3 & \beta_4 \end{vmatrix} = 0 \quad (18)$$

#### 4.1.2. Governing buckling equations for columns in vertically stacked sway modular frame

The model of sub-assemblage to extract the governing buckling equations for a column in a vertically stacked sway modular frame is comprised of column  $c_4$  restrained by two vertical inter-connections ( $S_{V1}$  and  $S_{V2}$ ), column  $c_2$  and  $c_6$ , and beams  $b_2$ ,  $b_4$ ,  $b_6$ , and  $b_8$ . The general equilibrium and compatibility equations, through the use of the slope-deflection method, stated in detail [6], result in:

$$\left[ 36G'_E G'_I \left( 1 + \sum_{k=E,I} \frac{SR_{kV}}{6G'_k} \right) + s_{ii} \left( \sum_{k=E,I} SR_{kV} + 6 \sum_{k=E,I} G'_k + s_{ii} \right) \right] \theta_I^2 + \left[ s_{ij} \left( \sum_{k=E,I} SR_{kV} + 6 \sum_{k=E,I} G'_k + 2s_{ii} \right) \right] \theta_I \theta_M + s_{ij}^2 \theta_M^2 - \frac{\Delta}{LC} \left[ (s_{ii} + s_{ij}) \sum_{k=E,I} SR_{kV} \theta_I + 6G'_E \sum_{k=i,j} s_{ik} \theta_I + s_{ii}^2 \theta_I + s_{ij}^2 \theta_M + s_{ii}s_{ij} \sum_{k=I,M} \theta_k \right] = 0 \quad (19)$$

$$\begin{aligned} & s_{ij}^2 \theta_I^2 + \left[ s_{ij} \left( \sum_{k=Q,M} SR_{kV} + 6 \sum_{k=Q,M} G'_k + 2s_{ii} \right) \right] \theta_I \theta_M + \left[ 36G'_M G'_Q \left( 1 + \sum_{k=Q,M} \frac{SR_{kV}}{6G'_k} \right) \right. \\ & \left. + s_{ii} \left( \sum_{k=Q,M} SR_{kV} + 6 \sum_{k=Q,M} G'_k + s_{ii} \right) \right] \theta_M^2 - \frac{\Delta}{LC} \left[ (s_{ii} + s_{ij}) \sum_{k=Q,M} SR_{kV} \theta_M + 6G'_Q \sum_{k=i,j} s_{ik} \theta_M + s_{ij}^2 \theta_I + s_{ii}^2 \theta_M + s_{ii}s_{ij} \sum_{k=I,M} \theta_k \right] = 0 \end{aligned} \quad (20)$$

$$\gamma_2 = 36G'_E G'_I \left( 1 + \sum_{k=E,I} \frac{SR_{kV}}{6G'_k} \right) + s_{ii} \left( \sum_{k=E,I} SR_{kV} + 6 \sum_{k=E,I} G'_k + s_{ii} \right) - \frac{(s_{ii} + s_{ij})^2}{2(s_{ii} + s_{ij}) - (kL_C)^2} \left( \sum_{k=E,I} SR_{kV} + 6G'_E + s_{ii} \right) \quad (25)$$

$$\begin{aligned} \gamma_1 \gamma_2 + \gamma_3 = s_{ij} \left( 2s_{ii} + 6 \sum_{k=E,I} G'_k + \sum_{k=E,I} SR_{IV} \right) - \frac{(s_{ii} + s_{ij})}{2(s_{ii} + s_{ij}) - (kL_C)^2} \left[ (s_{ii} + s_{ij}) \left( 6G'_E + \sum_{k=E,I} SR_{kV} \right) \right. \\ \left. + (s_{ii}) \right] \end{aligned} \quad (26)$$

where  $G'_I$  and  $G'_M$  are expressed by Eq. (9). The relative bending stiffness ratios of joints E and Q, and relative bending stiffness ratios of vertical inter-connections at nodes  $i$  ( $SR_{iV}$ ) are defined as:

$$G'_E = \frac{i_{b2}}{i_{c2}}, \quad G'_Q = \frac{i_{b8}}{i_{c6}} \quad (21)$$

$$SR_{EV} = \frac{R_{SV1}}{i_{c2}}, \quad SR_{IV} = \frac{R_{SV1}}{i_{c4}}, \quad SR_{MV} = \frac{R_{SV2}}{i_{c4}}, \quad SR_{QV} = \frac{R_{SV2}}{i_{c6}} \quad (22)$$

Eqs. (19) and (20) are rewritten in the simple form of Eqs. (23) and (24), respectively.

$$(\theta_I + \gamma_1 \theta_M) \times (\gamma_2 \theta_I + \gamma_3 \theta_M) = 0 \quad (23)$$

$$(\gamma_4 \theta_I + \theta_M) \times (\gamma_5 \theta_I + \gamma_6 \theta_M) = 0 \quad (24)$$

where the coefficients  $\gamma_1, \gamma_2, \gamma_3, \gamma_4, \gamma_5$ , and  $\gamma_6$  are

$$\gamma_1 \gamma_3 = s_{ij}^2 - \frac{(s_{ii} + s_{ij})(s_{ii}s_{ij} + s_{ij}^2)}{2(s_{ii} + s_{ij}) - (kL_C)^2} \quad (27)$$

$$\gamma_4 \gamma_5 = s_{ij}^2 - \frac{(s_{ii} + s_{ij})(s_{ii}s_{ij} + s_{ij}^2)}{2(s_{ii} + s_{ij}) - (kL_C)^2} \quad (28)$$

**Table 2**  
Flexibility coefficient  $\alpha_{bf}$  for different end conditions [29].

End conditions		$\alpha_{bf}$
End A	End B	
Rigid	Rigid	1
Rigid	Pinned	1/2
Rigid	Semi-rigid	$\left(1 + \frac{2EI_b}{L_b R_{kB}}\right) / \left(1 + \frac{4EI_b}{L_b R_{kB}}\right)$
Semi-rigid	Rigid	$1 / \left(1 + \frac{4EI_b}{L_b R_{kA}}\right)$
Semi-rigid	Pinned	$(1/2) / \left(1 + \frac{3EI_b}{L_b R_{kA}}\right)$
Semi-rigid	Semi-rigid	$\left(1 + \frac{2EI_b}{L_b R_{kB}}\right) / R^*$
Note: $R^*$		$\left(1 + \frac{4EI_b}{L_b R_{kA}}\right) \left(1 + \frac{4EI_b}{L_b R_{kB}}\right) - \left(\frac{EI_b}{L_b}\right)^2 \frac{4}{R_{kA} R_{kB}}$

one is associated with the buckling load and therefore acceptable. In order to solve the governing equations of buckling of columns, the MATLAB programming language and the *fslolve* function is employed. This function, based on a given initial point, uses an iterative method to find the solution of a linear/nonlinear equation system. The function uses three algorithms, including trust-region-dogleg, trust-region, and Levenberg-Marquardt, to solve the governing equations. Because it uses an iterative method, a step tolerance of 1e-16 is set to the function to ensure the accuracy of the obtained response. In addition to that, the acceptable responses are those that are greater than one due to the fact that the  $K$ -factor in sway frames cannot be less than one. To that, a restriction is imposed on the subroutine to ignore the responses which are less than one.

$$\gamma_4 \gamma_6 + \gamma_5 = s_{ij} \left( 2s_{ii} + 6 \sum_{k=M,Q} G'_k + \sum_{k=Q,M} SR_{kV} \right) - \frac{(s_{ii} + s_{ij})}{2(s_{ii} + s_{ij}) - (kL_C)^2} \left[ (s_{ii} + s_{ij}) \left( 6G'_Q \right. \right. \\ \left. \left. + \sum_{k=M,Q} SR_{kV} \right) + \left( \begin{array}{c} s_{ii} \\ \end{array} \right) \right] \quad (29)$$

$$\gamma_6 = 36G'_M G'_Q \left( 1 + \sum_{k=Q,M} \frac{SR_{kV}}{6G'_k} \right) + s_{ii} \left( \sum_{k=Q,M} SR_{kV} + 6 \sum_{k=Q,M} G'_k + s_{ii} \right) - \frac{(s_{ii} + s_{ij})^2}{2(s_{ii} + s_{ij}) - (kL_C)^2} \\ \left( \sum_{k=Q,M} SR_{kV} + 6G'_Q + s_{ii} \right) \quad (30)$$

The effective length factor, corresponding to buckling capacity, is obtained through Eqs. (31) to (34).

$$\begin{vmatrix} 1 & \gamma_1 \\ \gamma_4 & 1 \end{vmatrix} = 0 \quad (31)$$

$$\begin{vmatrix} 1 & \gamma_1 \\ \gamma_5 & \gamma_6 \end{vmatrix} = 0 \quad (32)$$

$$\begin{vmatrix} \gamma_2 & \gamma_3 \\ \gamma_4 & 1 \end{vmatrix} = 0 \quad (33)$$

$$\begin{vmatrix} \gamma_2 & \gamma_3 \\ \gamma_5 & \gamma_6 \end{vmatrix} = 0 \quad (34)$$

Eqs. (31) to (34) result in four answers, among which the maximum

#### 4.2. Numerical modelling of sway modular frame for displacement/drift analysis

To estimate the boundary values of rigid/semi-rigid zones and semi-rigid/pinned zones in sway corner-supported modular frames corresponding to their behaviour in the serviceability limit state, the general assemblage, shown in Fig. 3 is considered. Each module in this parametric model is made of columns, floor, and ceiling beams, in which they are assumed to be made of steel having a Square Hollow Section (SHS). The evaluation of the displacement and/or drift in a sway modular structure is a complicated procedure due to the presence of interconnections combined with the effects of intra-connections. One approach for the displacement analysis of these structures is the use of a simplified model, in which the displacement/drift of the structure can be obtained through virtual work. The second approach that can accurately capture the response of a structure, is the use of a finite element model (FEM) of the structure without the need for simplifications in finite

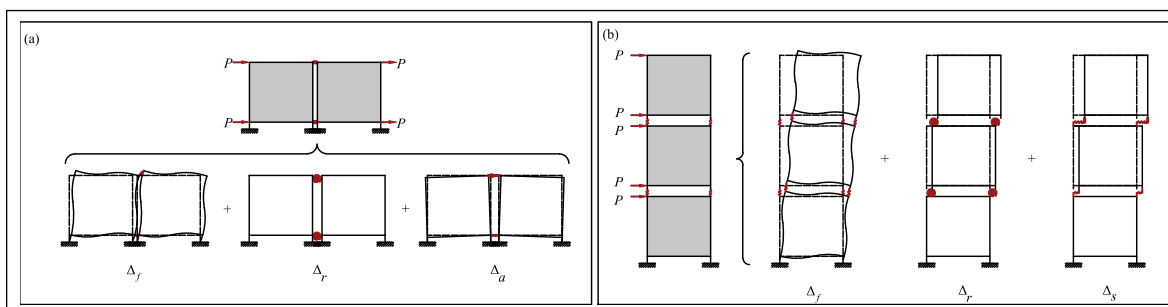


**Fig. 6.** (a) horizontally connected (b) vertically stacked sway modular frame.

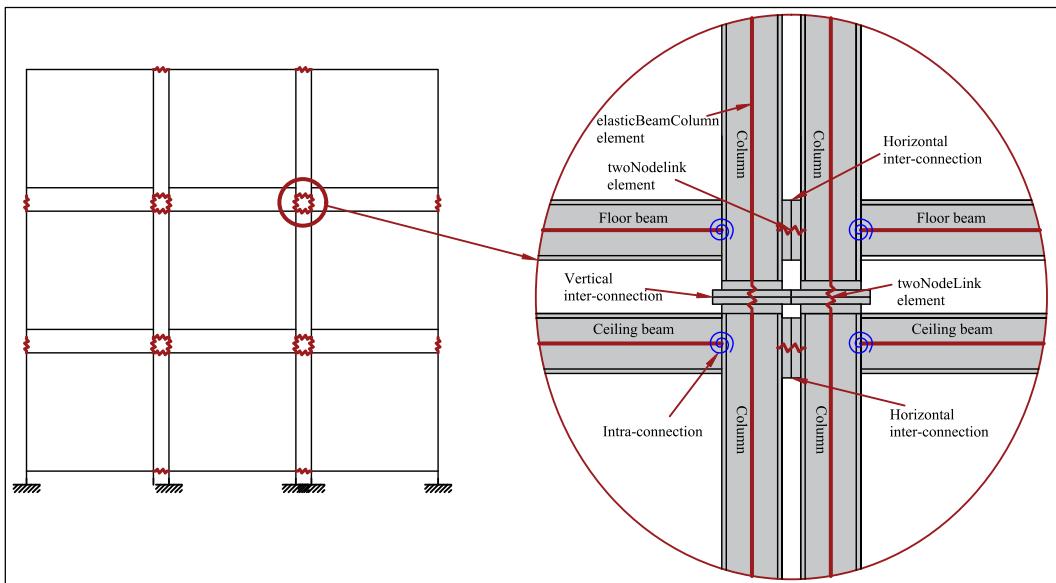


**Fig. 7.** Mathematical model of a joint in a sway modular frame in OpenSees.

element software. In this study, the second approach is adopted, and the finite element model of the modular structure has been performed in the OpenSees software framework [30]. This is an open-source software with a library providing different elements and springs with linear and nonlinear behaviour. In order to establish the classification system for horizontal and vertical inter-connections, it is assumed that the general assemblage is composed of various configurations of modules, including horizontally connected and vertically stacked modules. The two considered sub-assemblages with their deformed and undeformed shape under assumed horizontal loads are shown in Fig. 6 (a) and 5 (b), respectively.

The first sub-assemblage is composed of two horizontally connected modules through the use of horizontal inter-connections, tying the modules at floor and ceiling levels. The total deformation of the sub-assemblage is determined by taking into account of different components. The development of classification charts for rotational stiffness on inter-connections in serviceability limit state requires to recognize what factors can affect the deformation of the structure. Accordingly, the general subassemblage is distinguished into different components, hence in the next step, only the rotational components of inter-connections will be changed to provide the classification system. The total deformation of the structure under the imposed horizontal loads can be calculated as sum of the deformation due to the frame elements ( $\Delta_f$ ), the rotational component of horizontal inter-connections ( $\Delta_r$ ), and the axial component of inter-connections ( $\Delta_a$ ). The second sub-assemblage is made of three vertically connected sway modular

frames by the use of vertical inter-connections. The total deformation of the structure in the vertically connected sub-assemblage is obtained through the summation of the deformation of the frame elements ( $\Delta_f$ ), the deformation of vertical inter-connections due to their rotational components ( $\Delta_r$ ), and the deformation of vertical inter-connections due to their shear components ( $\Delta_s$ ). Fig. 7 shows the mathematical model of a joint in a modular frame for the displacement/drift analysis in the serviceability limit state in the OpenSees framework. The drift of the structure in the horizontally connected modular building is defined as the relative displacement of the ceiling of the structure to the displacement of the floor, which is divided by the height of the module. On the other hand, the second storey drift of the vertically stacked modular building is considered to develop the classification system for the vertical inter-connection in serviceability limit state. The drift of the second storey is determined based on the relative displacement of the second storey ceiling to its floor, which is divided by its height. The columns, floor, and ceiling beam elements of modules are modelled by elasticBeamColumn elements, which have an elastic behaviour. That is due to the fact that the serviceability limit state is related to the elastic behaviour of the structure. The intra-connections are assumed to have a linear behaviour and are modelled by discrete springs using zeroLength elements at the intersection of beams to columns. A large value is assigned to the shear and axial components of zeroLength elements to simulate the rigid behaviour corresponding to these components of intra-connections. Therefore, only the rotational component of intra-connection plays a role in the deformation of the frame. For the rotational component of intra-connections, it is determined based on the relative bending stiffness ratio of beams to intra-connections. In reality, the modules have a distance of 0.2 m in the horizontal and vertical directions due to the use of mechanical equipment and inter-connections. Therefore, in the mathematical model, the twoNodeLink elements are employed to simulate both horizontal and vertical inter-connections. This element may have linear or nonlinear behaviour. The use of twoNodeLink element allows the element to have a finite length. A large value is assigned to the in-plane axial and shear stiffness of inter-connections to simulate the rigid behaviour of these components resulting that these components have no contribution in the deformation of the structure. Hence, the classification charts are only provided for the rotational component. The diaphragm behaviour is considered for both ceiling and floor levels of each module by considering an equal degree-of-freedom for nodes at floors and ceilings in the horizontal direction using equalDOF in OpenSees. Therefore, both floor and ceilings have a

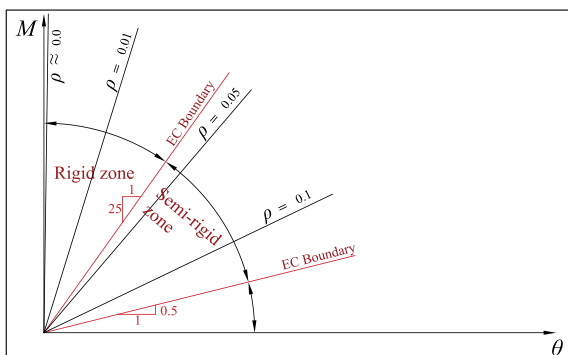


**Fig. 8.** Considered relative bending stiffness ratios of intra-connections.

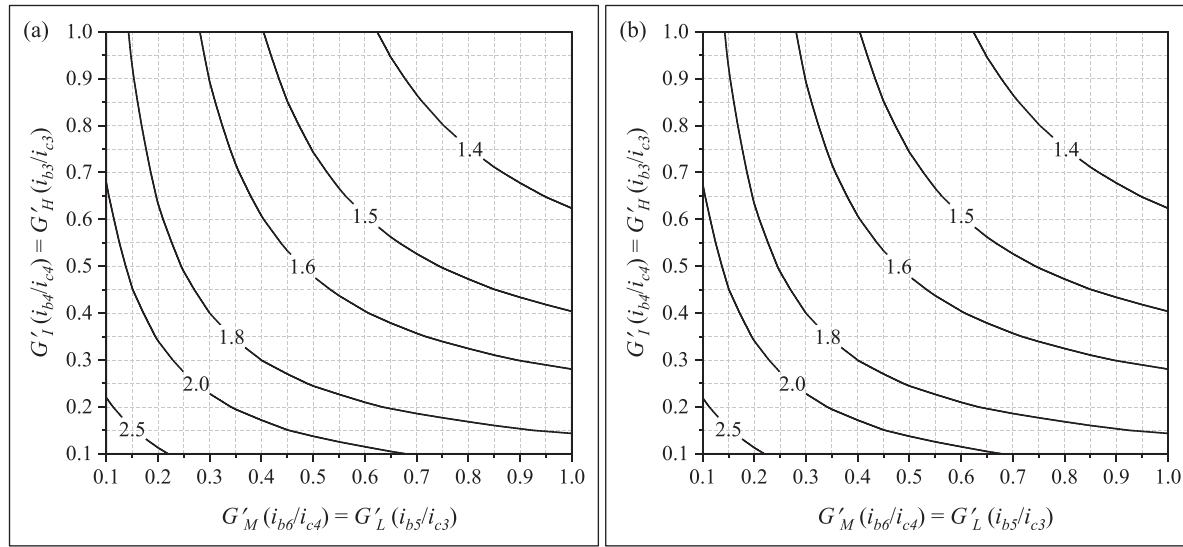


**Fig. 9.** Effective length factor of column  $c_4$  in the horizontally connected sway modular frame having rigid intra-connections and (a) rigid inter-connections (b) pinned inter-connections.

rigid diaphragm, which are typical practice in modular systems.

## 5. Development of the stiffness classification system and discussions

### 5.1. Classification of inter-connections based on the ultimate limit state

The classification system for the rotational stiffness of inter-connections, based on the ultimate limit state criterion, requires the calculation of the effective length factor, which is inversely proportional to the square root of buckling load of columns. The effective length factor, and therefore the buckling load of a column, is affected by different parameters, including the relative bending stiffness ratio of joints ( $G'$  ratios), the relative bending stiffness ratio of inter-connections ( $SR_H$  and  $SR_V$ ), and that of intra-connections ( $\rho$ ). In order to cover different mechanical properties of columns, floor, and ceiling beams for the classification system, the  $G'$  ratios of both floor and ceiling levels are varied from 0.1 to 1. Furthermore, four different stiffnesses for intra-connections have been considered to incorporate their rigidity on the

classification systems. The considered relative bending stiffnesses of intra-connections are:  $\rho = 0.0, 0.01, 0.05, 0.1$  (Fig. 8), in which the first two ones fall within the rigid zone and the rest lie in the semi-rigid zone, according to the classification system for beam-to-column connections suggested by Eurocode 3 [11]. Hence, the structural designers have more options to analyse and model the joint accurately in a sway modular frame.

#### 5.1.1. Classification system for horizontal inter-connections

In reality, during the design for manufacturing of modular frames, it is likely that modules with the same configurations and details of columns, floor, and ceiling beams are used in the plan of a structure. This results in the relative bending stiffness ratio of joint I becoming equal in value to that of joint H, i.e.,  $G'_I = G'_H$  (shown in Fig. 5 (a)), and the relative bending stiffness ratio of joint M becoming equal to that of joint L,  $G'_M = G'_L$ .

The effective length factor of column  $c_4$  for the case of rigid and pinned inter-connections is shown in three-dimensional contour charts, Fig. 9 (a) and (b), respectively. In this model, the intra-modular

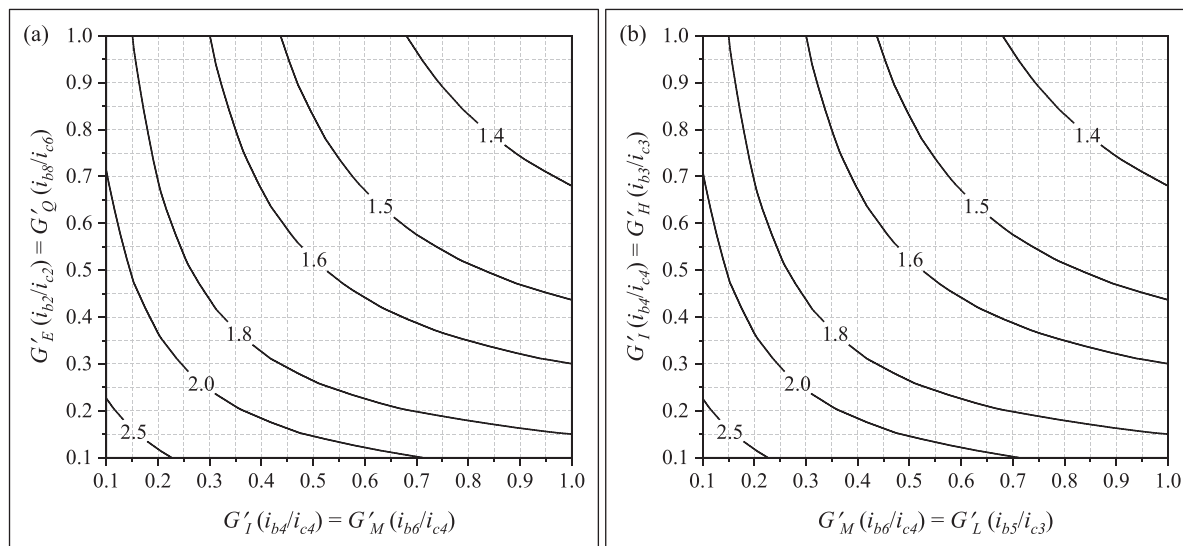


**Fig. 10.** Effective length factor of column  $c_4$  in the horizontally connected sway modular frame having intra-connections with relative bending stiffness ratio  $\rho = 0.01$  and (a) rigid inter-connections (b) pinned inter-connections.

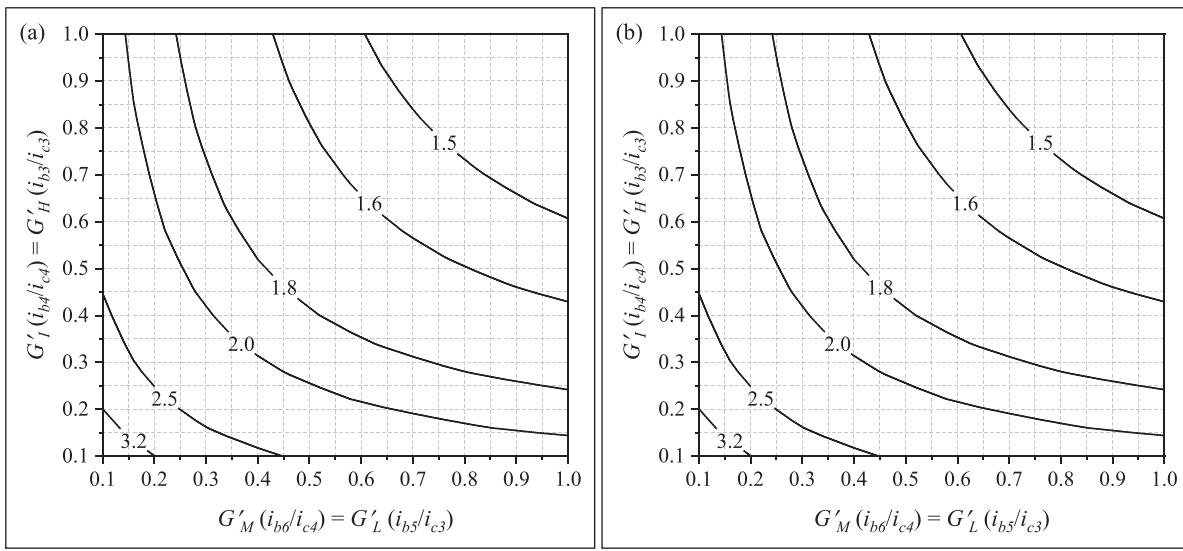


**Fig. 11.** Effective length factor of column  $c_4$  in the horizontally connected sway modular frame having intra-connections with relative bending stiffness ratio  $\rho = 0.05$  and (a) rigid inter-connection (b) pinned inter-connection.

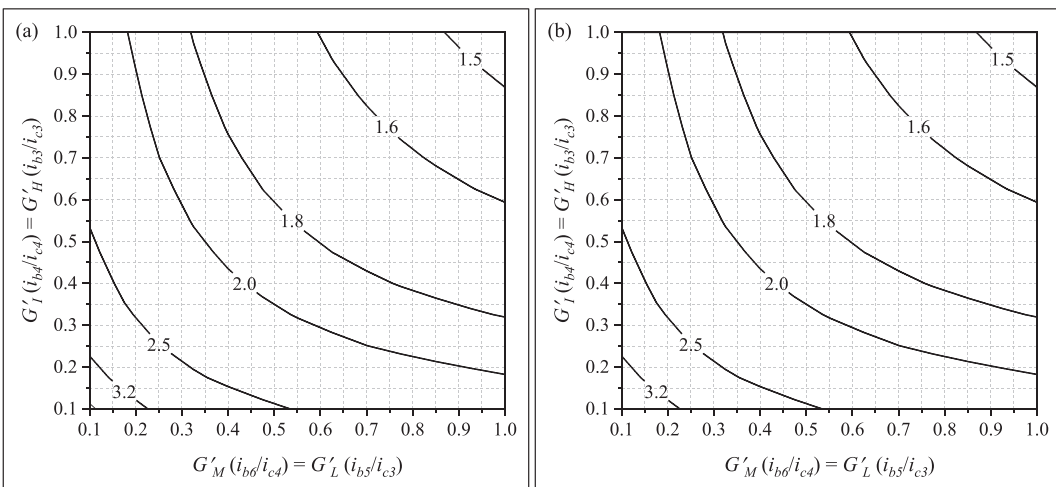


**Fig. 12.** Effective length factor of column  $c_4$  in the horizontally connected sway modular frame having intra-connection with relative bending stiffness ratio  $\rho = 0.1$  and (a) rigid inter-connections (b) pinned inter-connections.

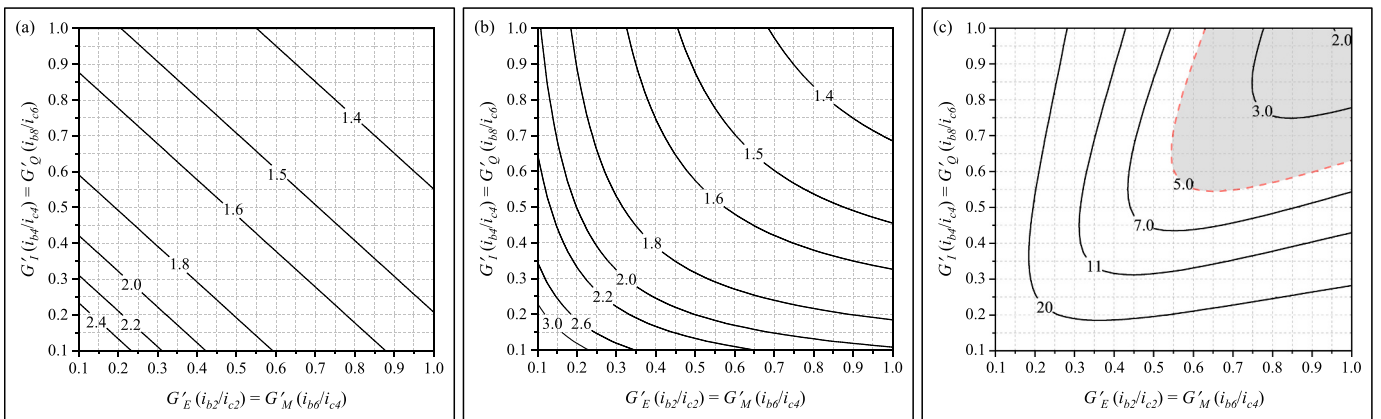


**Fig. 13.** Effective length factor of column  $c_4$  in the vertically stacked sway modular frame having rigid intra-connections and (a) rigid inter-connections (b) pinned inter-connections (c)  $\delta_K$  for rigid and pinned behaviour of inter-connections.

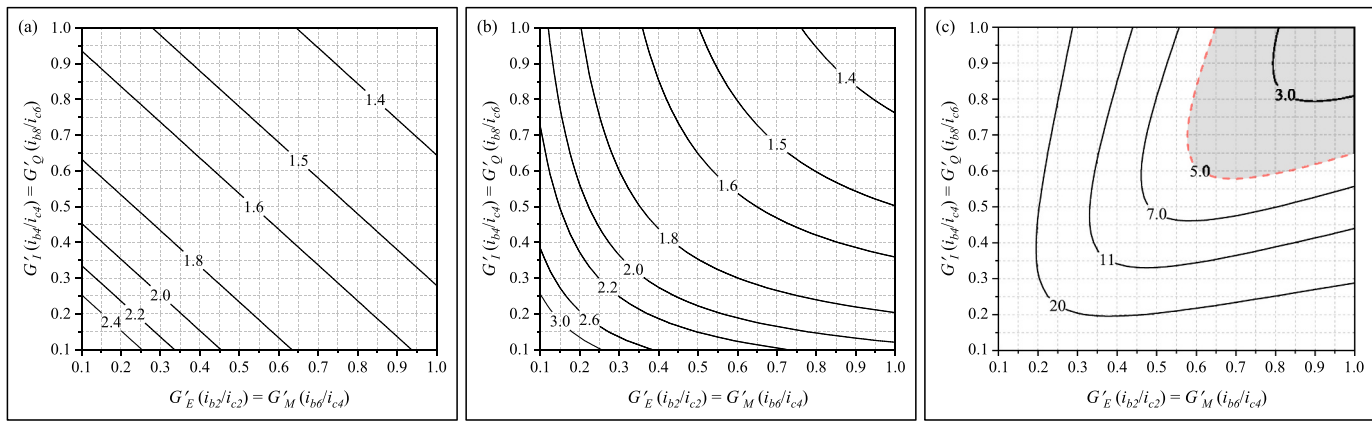


**Fig. 14.** Effective length factor of column  $c_4$  in the vertically stacked sway modular frame having intra-connections with relative bending stiffness ratio  $\rho = 0.01$  and (a) rigid inter-connections (b) pinned inter-connections (c)  $\delta_K$  for rigid and pinned behaviour of inter-connections.

connection is assumed to have a rigid behaviour ( $\rho \approx 0.0$ ). The aim is to obtain the stiffness of horizontal inter-connections, which results in a 5% and 75% reduction in the buckling capacity of column  $c_4$ . Therefore, in the next stage, the boundary values corresponding to rigid/semi-rigid zones as well as that for semi-rigid/nominally-pinned zones can be determined. In order to have a better understanding of how the stiffness of inter-connections influences the buckling capacity, the buckling capacity, the difference percentage of rigid and pinned behaviour of inter-connections is defined as:

$$\delta_K = \left| \left( \frac{\frac{1}{K_R^2} - \frac{1}{K_P^2}}{\frac{1}{K_R^2}} \right) \right| \times 100 \quad (35)$$

The equation shows for  $\delta_K$  less than 5%, no classification system is required. The rigid behaviour can easily be modelled by considering a large value (say 1e14) for the stiffness of inter-connections, and the pinned behaviour can be modelled by assuming a small value, e.g., 1e-14 to the stiffness of inter-connections. Fig. 9 (a) and 8 (b) illustrate that the  $K$ -factor of column  $c_4$  varies from 1.4 to 2.5 for different relative bending stiffness ratios of floor and ceiling to column, when inter-connections have a rigid and pinned behaviour. The former corresponds to the higher value of  $G'$ , and the latter is associated with the lower values of  $G'$ . The charts indicate that the  $K$ -factor is not affected by the behaviour of inter-connections, and it remains constant for both rigid and pinned behaviour of inter-connections ( $\delta_K = 0$ ). This shows that no boundary values are required to be determined when inter-connections have a rigid behaviour. In this model, the behaviour of horizontal inter-

connections can be modelled by a rigid element.

In order to determine the influence of the flexibility of intra-connections on the effective length factor, and the classification system, the flexibility of intra-connections is increased by  $\rho = 0.01$ . The  $K$ -factors of column  $c_4$  corresponding to rigid and pinned behaviour of horizontal inter-connections are plotted in Fig. 10 (a) and 9 (b), respectively. The obtained responses suggest that the  $K$ -factor varies from 1.4 to 2.5 for different  $G'$  ratios of floor and ceiling, which is almost the same as those of the rigid behaviour of intra-connections ( $\rho \approx 0.0$ ). The comparison of the  $K$ -factor obtained from assuming rigid inter-connections with the ones of pinned inter-connections illustrates that the horizontal inter-connections have no effect on the buckling capacity of the column, and it remains constant for both considered behaviour. Therefore, no classification system is required for the horizontal inter-connection when the intra-connections have a rigid behaviour with  $\rho = 0.01$ .

In the next stage, the flexibility of intra-connections is increased to  $\rho = 0.05$ , which falls within the semi-rigid zone based on the classification system for intra-connections proposed by Eurocode 3. The effective length factor of column  $c_4$  corresponding to rigid and pinned inter-connections are shown in Fig. 11 (a) and 10 (b), respectively. The obtained responses indicate that the use of semi-rigid intra-connections increases the effective length factor of the column, in which it varies from 1.5 to 3.2 in both rigid and pinned behaviour of inter-connections. The former corresponds to the higher values of  $G'$  ratios, and the latter corresponds to the lower values of  $G'$  ratios. Hence, the buckling capacity of the column decreases compared to the use of rigid intra-connections. In fact, the introduction of flexibility at ends of beam

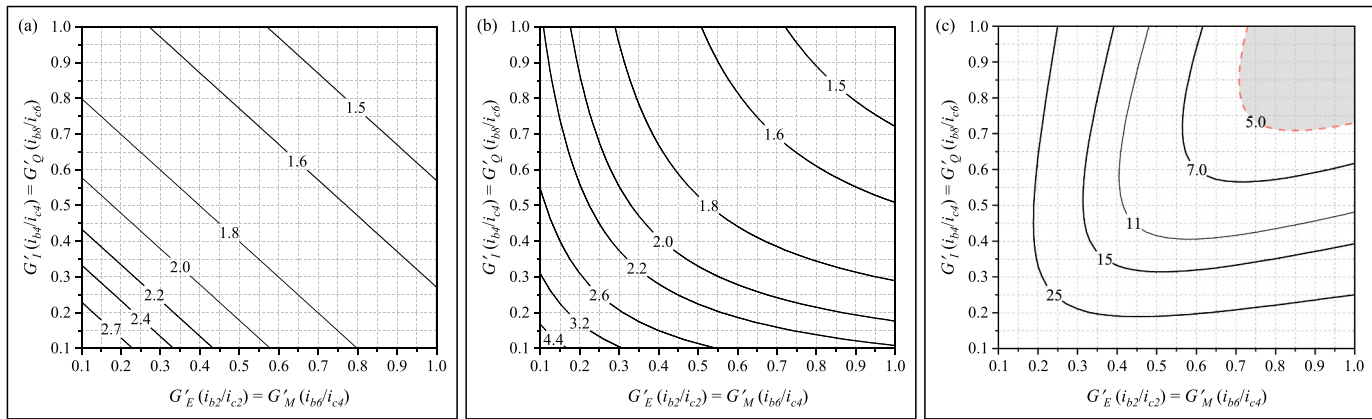


**Fig. 15.** Effective length factor of column  $c_4$  in the vertically stacked sway modular frame having intra-connections with relative bending stiffness ratio  $\rho = 0.05$  and (a) rigid inter-connections (b) pinned inter-connections (c)  $\delta_K$  for rigid and pinned behaviour of inter-connections.

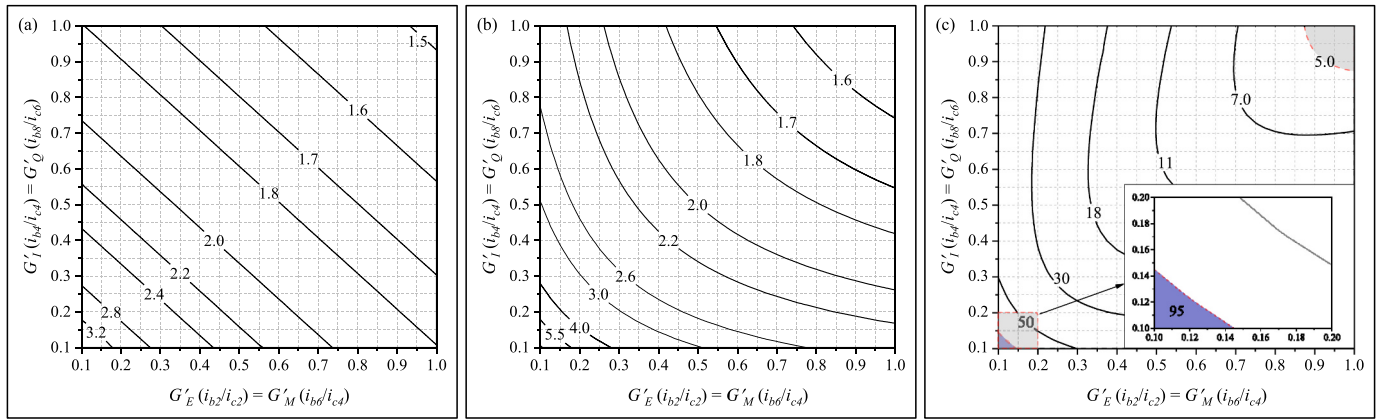


**Fig. 16.** Effective length factor of column  $c_4$  in the vertically stacked sway modular frame having intra-connections with relative bending stiffness ratio  $\rho = 0.1$  and (a) rigid inter-connections (b) pinned inter-connections (c)  $\delta_K$  for rigid and pinned behaviour of inter-connections.

elements by the employment of semi-rigid intra-connections, results in the decrease of buckling capacity of the column. Moreover, the comparison of rigid and pinned behaviour of inter-connections indicates that the rotational stiffness of horizontal inter-connections has no effect on the  $K$ -factor, meaning that no classification is needed for the rotational

stiffness of the horizontal inter-connection when a semi-rigid intra-modular with  $\rho = 0.05$  is employed in the structure.

At the final stage, the flexibility of intra-connections is increased to  $\rho = 0.1$ , indicating that an intra-connection with semi-rigid behaviour is used in the sway modular frame. The response of the  $K$ -factor for two

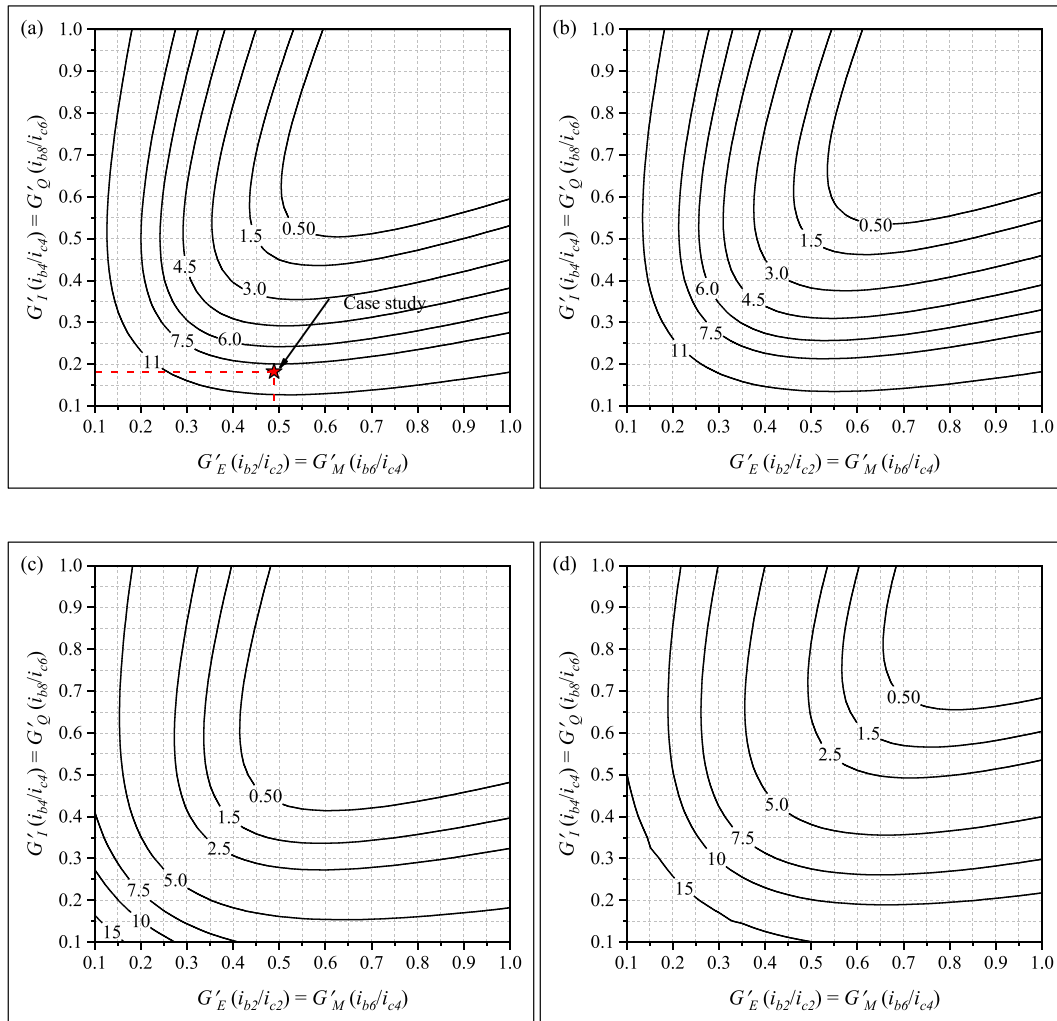


**Fig. 17.** Rigid/Semi-rigid boundary zones, based on ultimate limit state of inter-connection for (a) rigid intra-connections ( $\rho \approx 0.0$ ); (b) intra-connections with relative bending stiffness ratio of  $\rho = 0.01$  (c) intra-connections with relative bending stiffness ratio of  $\rho = 0.05$  (d) intra-connections with relative bending stiffness ratio of  $\rho = 0.1$ .

cases of rigid and pinned behaviour of horizontal inter-connections is plotted in Fig. 12.

The comparison of the results indicates that a similar trend is observed when semi-rigid intra-connections are used in the structure. That is, the flexibility of horizontal inter-connections does not influence the behaviour of the structure in the ultimate limit state, and no classification is required for the rotational stiffness of horizontal interconnection. As a result, the rotational stiffness of horizontal inter-connections can be ignored during the modelling, analysing, and designing of a sway modular frame, and it can be modelled by a rigid behaviour element regardless of the rigidity of intra-connections. In fact, the main reason that the horizontal inter-connection has no effect on the buckling capacity of columns can attributed to the assumption that two adjacent modular units with a similar configuration is used for the classification system. That is, when a similar configuration is employed, both modular units have a similar deformation under critical axial load. Therefore, the horizontal inter-connection has no relative deformation, leading to a zero moment in the horizontal inter-connection regardless of its stiffness. Hence, the effective length factor of column in this situation remains constant for both rigid and pinned behaviour of horizontal inter-connection.

### 5.1.2. Classification system for vertical inter-connections

One of the advantages of modular frames is the use of typical units for various designs, and hence in reality, during the design process of a building, modules with similar configurations are used in height. This results in an equal relative bending stiffness ratio at floor levels, i.e.,  $G'_E = G'_M$  (shown in Fig. 5 (b)), and equal relative bending stiffness ratio at ceiling levels, i.e.,  $G'_I = G'_Q$ . Therefore, the proposed classification systems for vertical inter-connections are valid when the relative bending stiffness ratios of node E equals that of node M, and the relative bending stiffness ratio corresponding to node I equal to that of node Q, respectively.

The effective length factor of column  $c_4$  corresponding to rigid and pinned behaviour of inter-connections and rigid intra-connections (i.e.,  $\rho \approx 0.0$ ) are shown in Fig. 13 (a) and 12 (b). Similar to the previous section, the rigid and pinned behaviours are modelled by assigning large and small values to the rotational stiffness of inter-connections, respectively. The results are plotted in three-dimensional contour charts in order to obtain the stiffness ratio resulting in a 5% and 75% reduction in buckling capacity of the column  $c_4$ . Therefore, in the next stage, the boundary values corresponding to the rigid/semi-rigid zones

and semi-rigid/pinned zones are respectively determined.

The results indicate that the  $K$ -factor varies between 1.4 and 2.4 when inter-connections are assumed to behave rigidly. On the other hand, considering the pinned behaviour of inter-connections leads to an increase in the  $K$ -factor, in which it varies from 1.4 to 3. The former corresponds to the higher values of  $G'$  ratios and the latter corresponds to the lower values of  $G'$  ratios. The comparison of the rigid and pinned behaviour of inter-connections, shown in Fig. 13 (c), indicates that the  $\delta_K$  varies from 2%, and in some cases, it reaches to 20%. The  $\delta_K$  corresponding to a 5% change in the buckling capacity of the column is highlighted by a red dashed line in the figure. The figure illustrates that no classification system is needed for  $G'$  ratios that lie within the grey zone, where the  $\delta_K$  is less than 5%. In these cases, the behaviour of inter-connections has no effect on the effective length factor, therefore, buckling capacity. Moreover, the maximum  $\delta_K$  is about 20%, and is far less than 75% which is set to determine the boundary values of the semi-rigid/pinned zones. So, vertical inter-connections may have a rigid or semi-rigid behaviour in a sway modular frame depending on the relative bending stiffness ratios at floor and ceiling levels.

In order to study the effect of the stiffness of intra-connections on the classification system, the flexibility of intra-connections is increased by 0.01 (i.e.,  $\rho = 0.01$ ). Although the rigidity of the intra-connections is decreased, it remains in the rigid zone. The effective length factors of column  $c_4$  considering rigid and pinned behaviour of vertical inter-connections are shown in Fig. 14 (a) and 13 (b), respectively. The comparison of the obtained effective length factor with the ones of rigid intra-connections (Fig. 13 (a) and 12 (b)) indicates that a similar response is obtained for the effective length factor, meaning that the increase of the flexibility of intra-connections has no considerable effect on the  $K$ -factor. The  $K$ -factors vary from 1.4 to 2.4 when inter-connections have a rigid behaviour depending on the relative bending stiffness ratio of floor and ceiling levels. Turning the behaviour of inter-connections from rigid to pinned behaviour leads to an increase of the effective length factor, in which it varies from 1.4 to 3.0. The comparison of the rigid and pinned behaviour of inter-connections, shown in Fig. 14 (c), indicates that the  $\delta_K$  varies from 3% to 20% depending on the  $G'$  ratios. For the  $\delta_K$  less than 5%, indicated by the grey zone, the rigidity of inter-connections has no effect on the behaviour of the structure in the ultimate limit state, and the joint can be modelled as a continuous joint. On the other hand, for those relative bending stiffness ratios in which the  $\delta_K$  is more than 5%, the inter-connections' influence should be considered in the structure analysis. In addition to that, the highest value of the  $\delta_K$  is far less than 75% which is set to obtain the boundary values of the semi-rigid/nominally-pinned zones. Hence, inter-connection may have two behaviours, rigid or semi-rigid.

As intra-connections become more flexible (i.e.,  $\rho = 0.05$ ), the effective length factor of column  $c_4$  is affected in both rigid and pinned behaviour of inter-connections. Fig. 15 (a) and 14 (b) shows that as the flexibility of intra-connections increases the effective length factor of the column goes up, leading to a decrease in buckling capacity. The comparison of the results of the rigid behaviour of inter-connections with pinned ones, shown in Fig. 15 (c), implies that the  $\delta_K$  varies by up to 25%, which is slightly more than that of the rigid behaviour of intra-connections, shown in Fig. 13 (c). However, the maximum  $\delta_K$  is still less than 75%, which is set to estimate the boundary value of the semi-rigid/nominally-pinned zones. The grey zone, corresponding to the  $\delta_K$  less than 5%, clarifies that vertical inter-connections have no significant effect on the buckling capacity, so their modelling becomes unnecessary. For those  $\delta_K$  more than 5%, the classification should be presented; and depends on the relative bending stiffness of inter-connections, it can be modelled as a rigid or semi-rigid inter-connections.

Finally, the value of 0.1 is assigned to the relative bending stiffness ratio of intra-connections to reduce the rigidity of the intra-connections, representing a semi-rigid behaviour. The effective length factor of column  $c_4$  corresponding to rigid and pinned behaviour of inter-connections is illustrated in Fig. 16 (a) and 15 (b). With reference to

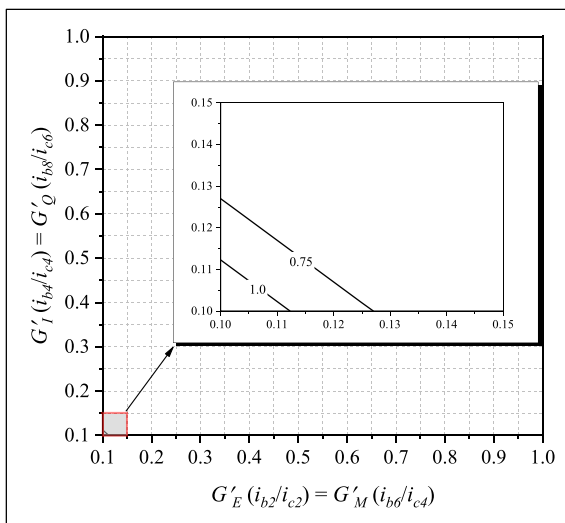


**Fig. 18.** Semi-rigid/pinned boundary zone of vertical inter-connections based on the ultimate limit state when intra-connections have a relative bending stiffness ratio of  $\rho = 0.1$ .

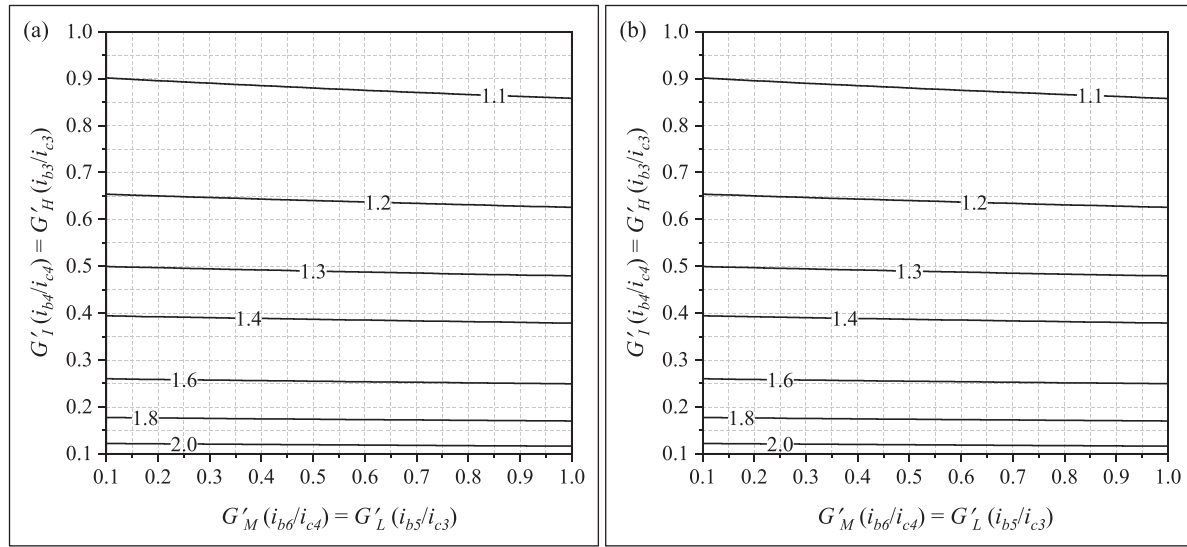


**Fig. 19.** The drift of the horizontally connected sub-assemblage having rigid intra-connections (a) rigid inter-connections (b) pinned inter-connections.

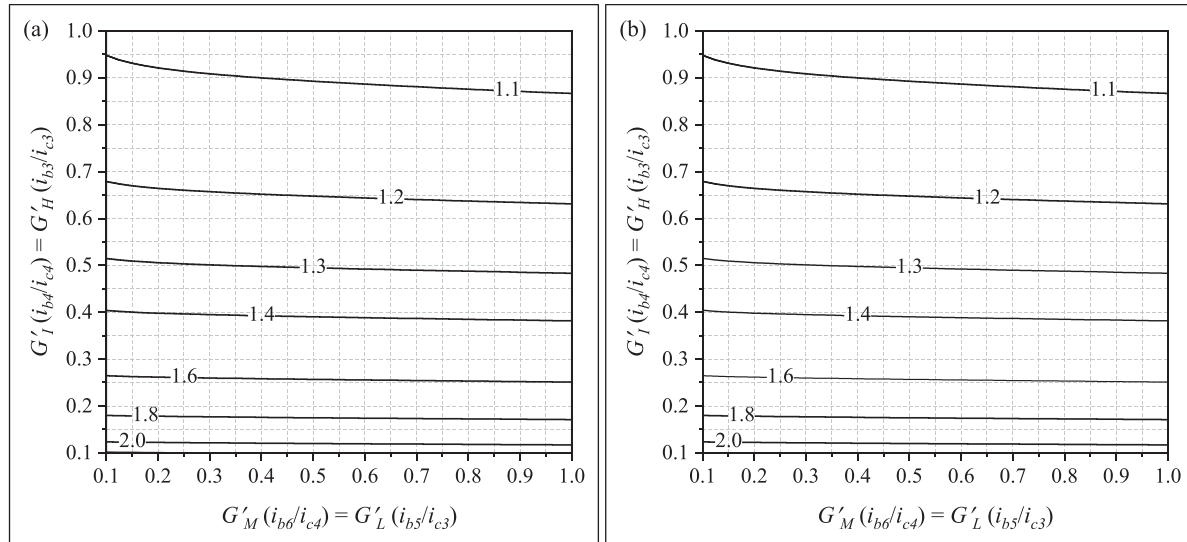


**Fig. 20.** The drift of the horizontally connected sub-assemblage having intra-connections with relative bending stiffness ratio  $\rho = 0.01$  and (a) rigid inter-connections (b) pinned inter-connections.

**Fig. 16** (a) and 15 (b), the incorporation of a more flexible intra-connections leads to an increase in the effective length factor, therefore, the reduction of buckling capacity of the column. For the rigid behaviour of inter-connections, the charts suggest that the effective length factor changes from 1.5 to 3.2, while for the pinned behaviour of inter-connections, the effective length factor varies between 1.6 and 5.5 depending on the configuration of floors and ceilings. **Fig. 16** (c) shows the  $\delta_K$  parameter when the behaviour of the inter-connection turns from rigid to pinned behaviour. The  $\delta_K$  varies from 3%, corresponding to higher values of relative bending stiffness ratios, up to 95%, corresponding to lower values of relative bending stiffness ratios of floor and ceiling. The shrinkage of the grey zone illustrates that in most cases, the inter-connections' behaviour changes buckling capacity of the column by more than 5%. Therefore, the classification should be performed to determine the boundary values corresponding to the rigid/semi-rigid zones. On the other hand, the presence of the blue zone, which corresponds to 75% and more reduction in the buckling capacity of column  $c_4$ , indicates that some rotational stiffness of inter-connections behaves as a pinned inter-connections. So, it is needed to determine the boundary

values for the semi-rigid/nominally-pinned zones.

The conducted parametric study helps to establish and develop the boundary values of rigid/semi-rigid and semi-rigid/nominally-pinned zones, respectively. Using the charts above and employing Eqs. (1) and (4), the boundaries of the rigid and semi-rigid zones for vertical inter-connections in terms of relative stiffness of inter-connections to column in sway corner-supported modular frames can be extracted for the ultimate limit state criterion. The boundary values corresponding to rigid/semi-rigid zones for the considered intra-connections are presented in **Fig. 17** (a) to (d). The charts indicate the minimum required rotational stiffness of vertical inter-connections, which results in 5% drop in buckling capacity of the column compared to the rigid behaviour of vertical inter-connections. The provided charts illustrates the required minimum relative bending stiffness ratios of vertical inter-connections to be classified as a rigid inter-connection. As an example, for the case study, highlighted in **Fig. 17** (a), if an inter-connection has a relative bending stiffness ratio higher than 7.8, it is classified as a rigid connection and can be modelled by a continuous joint in the mathematical model of a structure which significantly simplifies the modelling

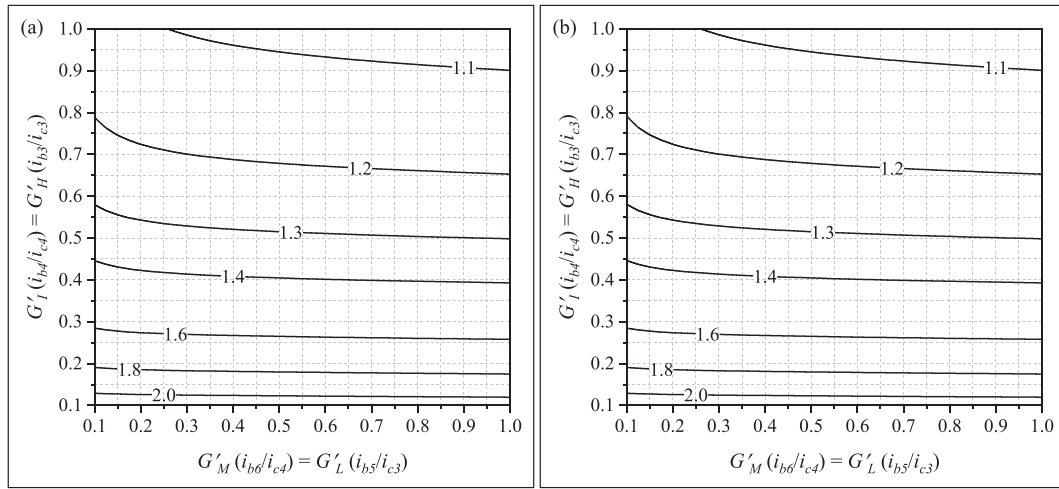


**Fig. 21.** The drift of the horizontally connected sub-assemblage having intra-connections with relative bending stiffness ratio  $\rho = 0.05$  and (a) rigid inter-connections (b) pinned inter-connections.

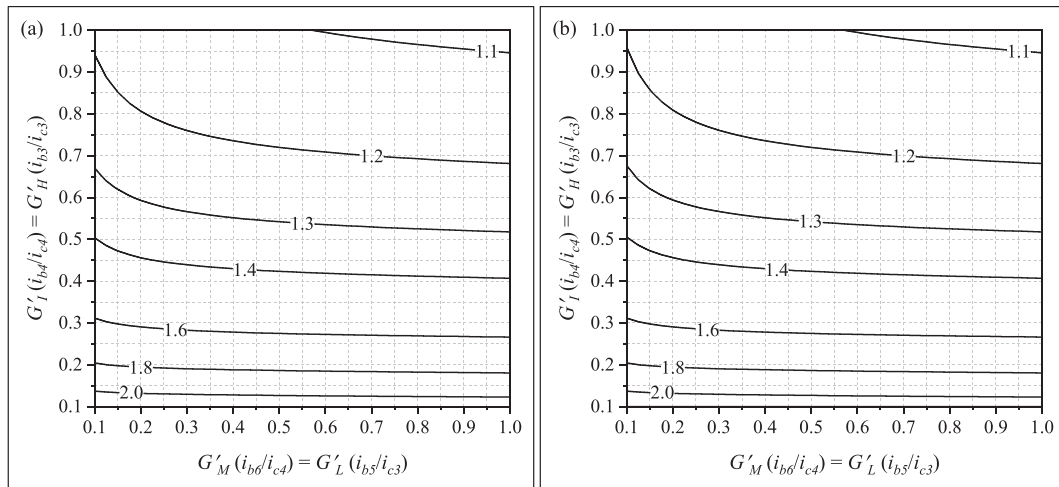


**Fig. 22.** The drift of node M of the horizontally connected sub-assemblage having intra-connection with relative bending stiffness ratio  $\rho = 0.1$  and (a) rigid inter-connections (b) pinned inter-connections.

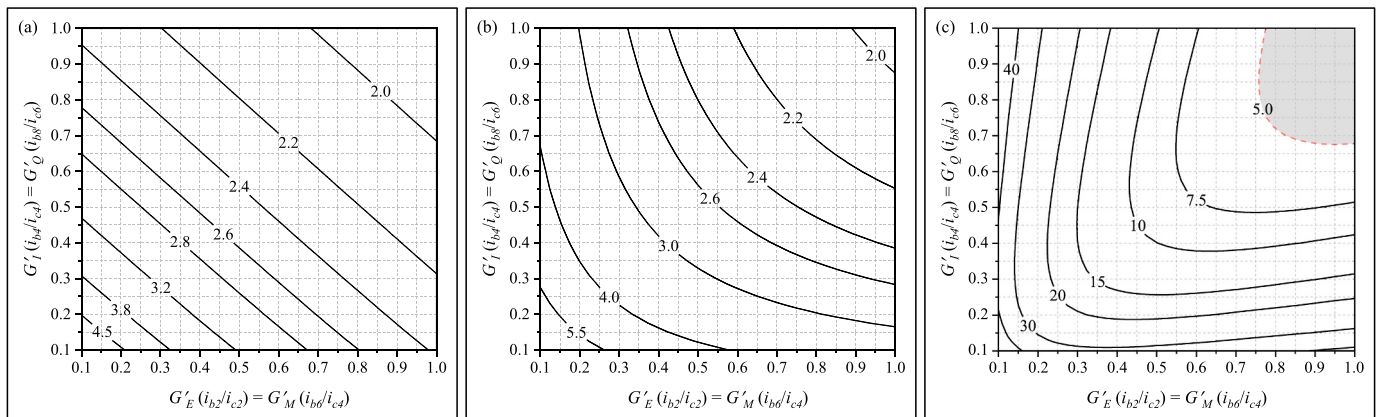


**Fig. 23.** The drift of the second storey of the vertically stacked sub-assemblage having rigid intra-connections and (a) rigid inter-connections (b) pinned inter-connections (c)  $\delta_D$  of drift for rigid and pinned behaviour of inter-connections.

procedure of a modular frame. On the other hand, for the relative bending stiffness ratio of inter-connections smaller than 7.8, the joint should be modelled as a semi-rigid joint in the modelling of a structure,

and the influence of the stiffness of vertical inter-connections on the static and dynamic responses of the structure should be considered in the design process. The process on how to use the classification charts are

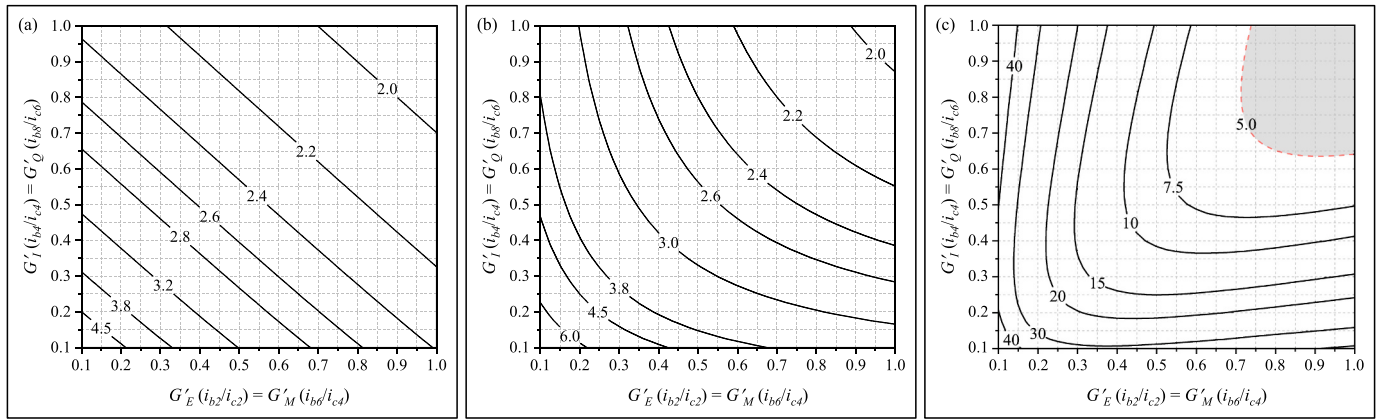


**Fig. 24.** The drift of the second storey of the vertically stacked sub-assemblage having intra-connection with relative bending stiffness ratio  $\rho = 0.01$  and (a) rigid inter-connections (b) pinned inter-connections (c)  $\delta_D$  of drift for rigid and pinned inter-connections.

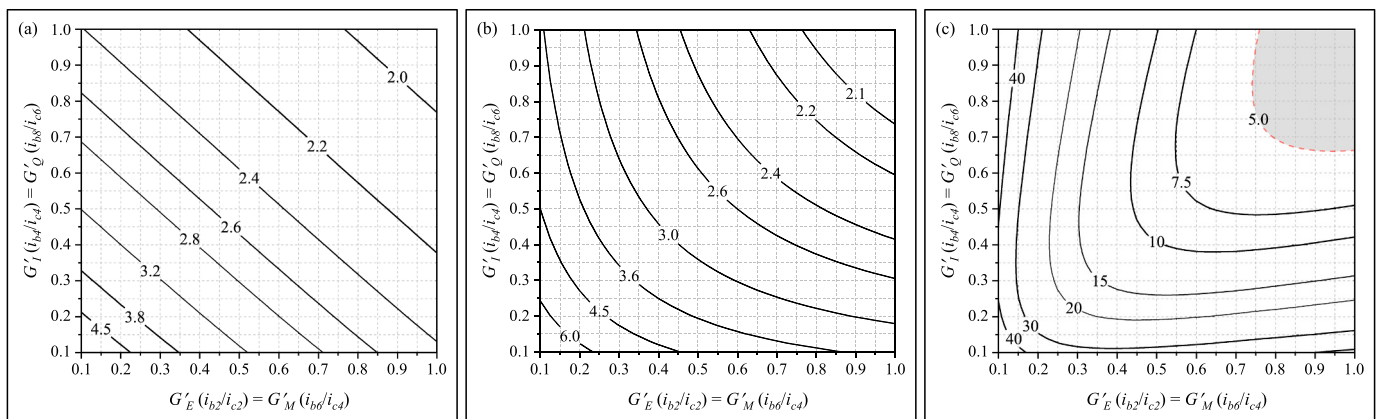


**Fig. 25.** The drift of the second storey of the vertically stacked sub-assemblage having intra-connection with relative bending stiffness ratio  $\rho = 0.05$  and (a) rigid inter-connections (b) pinned inter-connections (c)  $\delta_D$  of drift for rigid and pinned inter-connections.

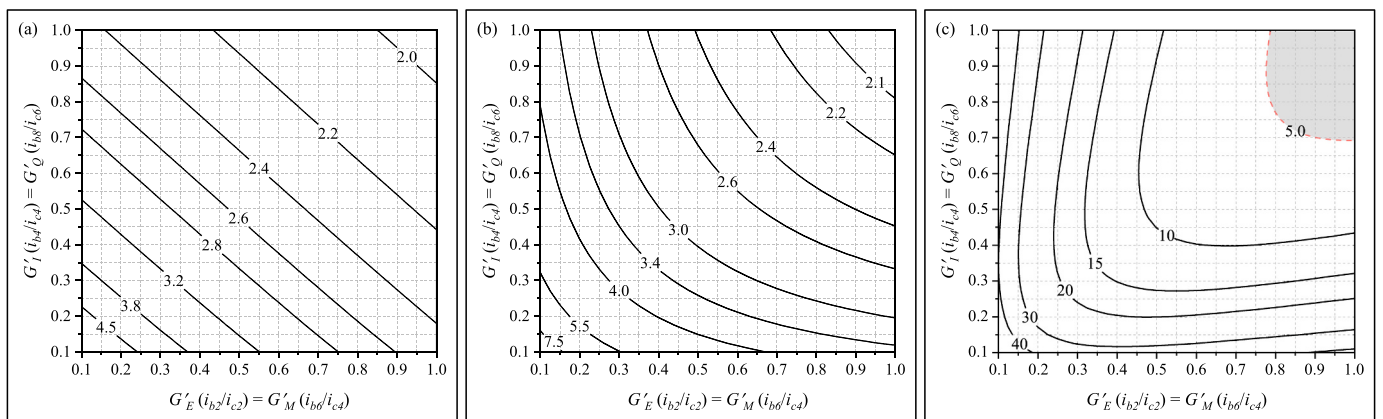


**Fig. 26.** The drift of the second storey of the vertically stacked sub-assemblage having intra-connection with relative stiffness ratio  $\rho = 0.1$  and (a) rigid inter-connections (b) pinned inter-connections (c)  $\delta_D$  of drift for rigid and pinned inter-connections.

more explained in the case study example and design recommendations throughout a flowchart.

Because in most of the above cases (except for  $\rho = 0.1$ ), the maximum obtained  $\delta_K$  is less than 75%, there is no need to determine the boundary values corresponding to semi-rigid/nominally-pinned zones; i.e. they behave either as a rigid inter-connection or semi-rigid inter-connection. However, the  $\delta_K$  can reach to 75% and more in some configurations of the case  $\rho = 0.1$ . So, the boundary values corresponding to semi-rigid/

nominally-pinned zones are required to be determined, which is depicted in Fig. 18. The figure indicates that the boundary values vary between 0.25 and 1 depending on the configuration of the structure.

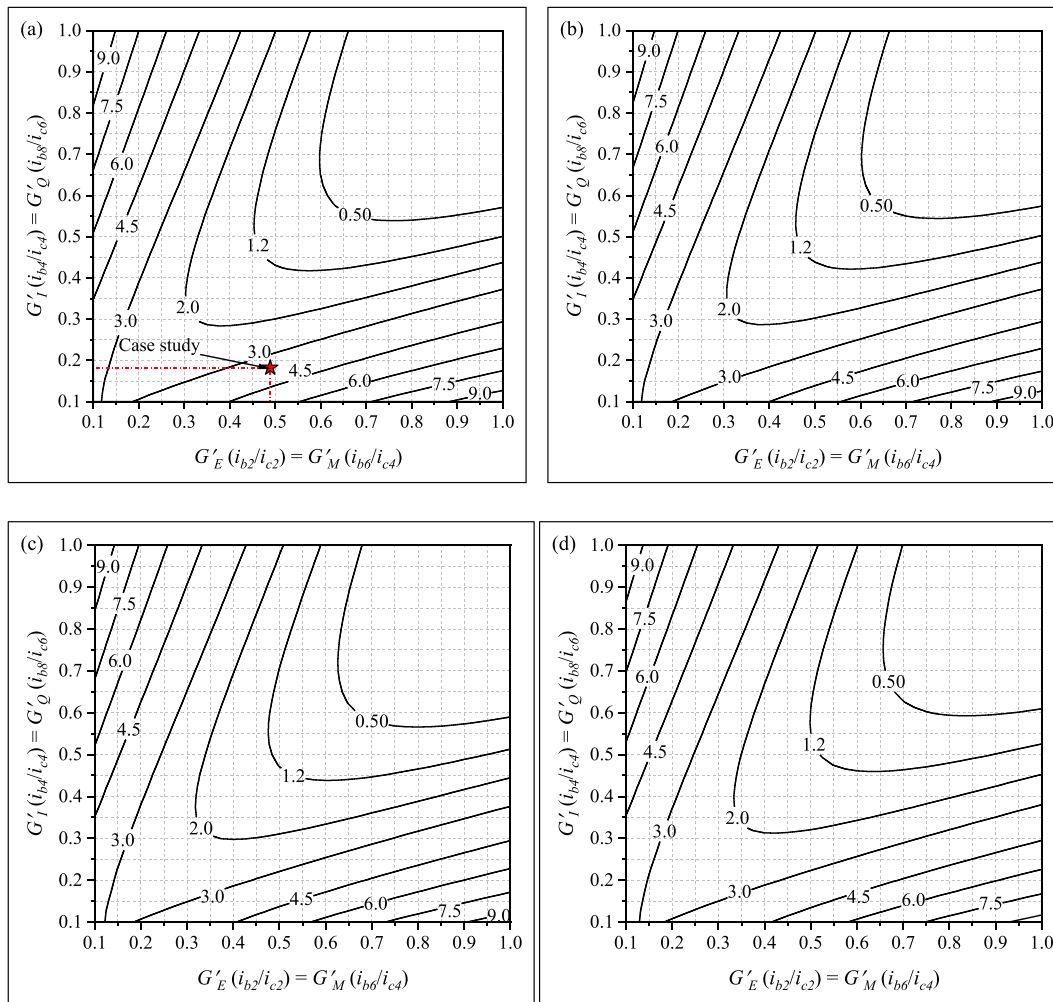


**Fig. 27.** Rigid/Semi-rigid boundary zones, based on the serviceability limit state of vertical inter-connection for (a) rigid intra-connections ( $\rho \approx 0.0$ ); (b) intra-connections with relative bending stiffness ratio of  $\rho = 0.01$  (c) intra-connections with relative bending stiffness ratio of  $\rho = 0.05$  (d) intra-connections with relative bending stiffness ratio of  $\rho = 0.1$ .

## 5.2. Classification of inter-connections based on the serviceability limit state

### 5.2.1. Classification of horizontal inter-connections

To establish a classification system for horizontal inter-connections

in the serviceability limit state, a set of horizontal loads is imposed to the horizontally connected modular structure shown in Fig. 6 (a). Concentrated loads are imposed to different nodes at both floor and ceiling levels, and the drift of the modules is captured to investigate the influence of rotational stiffness of horizontal inter-connections on the

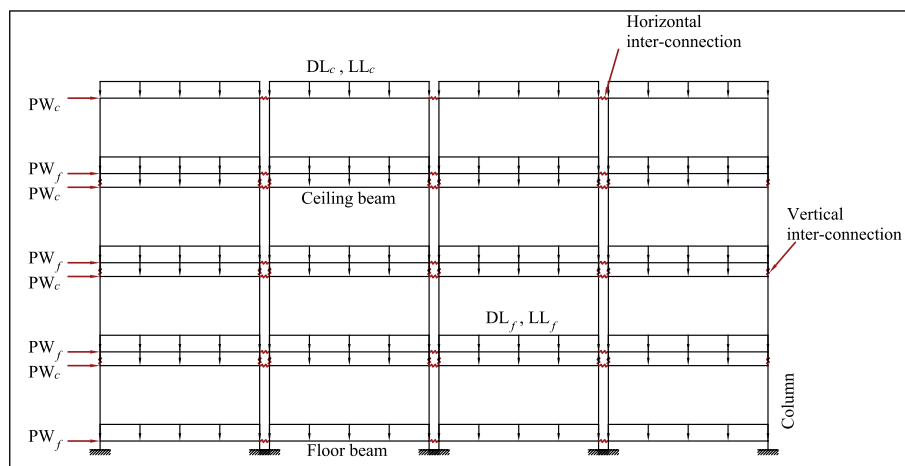


**Fig. 28.** The elevation view of the considered sway modular frame for the numerical study.

drift. Similar to the ultimate limit state, the difference percentage of drift in rigid and pinned behaviour of inter-connections is defined as:

$$\delta_D = \left| \left( \frac{\Delta_R - \Delta_{SR}}{\Delta_R} \right) \right| \times 100 \quad (35)$$

The drift of the modular structure for rigid and pinned behaviour of the horizontal inter-connections, while a rigid behaviour is assigned to intra-connections ( $\rho \approx 0.0$ ) is shown in Fig. 19 (a) and 18 (b). The response of the structure in rigid and pinned behaviour of horizontal inter-connections indicates that the rotational stiffness of horizontal inter-connections does not affect the drift of the structure. This shows that the rigidity of the horizontal inter-connections can be ignored in the modelling of the structure under the serviceability limit state.

The flexibility of intra-connections is increased by 0.01 to evaluate its rigidity on the classification system of horizontal inter-connections. Fig. 20 (a) and 19 (b) show the drift of the horizontally connected modules using rigid and pinned behaviour of horizontal inter-connections, respectively. The obtained responses show that a similar drift is obtained in both rigid and pinned behaviour of inter-connections. Therefore, no classification is required for the horizontal inter-connections for the serviceability limit state.

At the next stage, the flexibility of intra-connections is increased to  $\rho = 0.05$ , in which it is fitted in the semi-rigid zone based on the classification of beam-to-column connections. The drift results of the structure, depicted in Fig. 21 (a) and 20 (b), illustrate that the behaviour of inter-connections has no influence on the response of the structure, and it is constant regardless of the stiffness of horizontal inter-connections. So, no classification is required for this case.

Finally,  $\rho$  of 0.1 is assigned to the relative bending stiffness of intra-connections, and the drift of the structure is measured during the change of stiffness of horizontal inter-connections. Fig. 22 (a) and 21 (b) show the drift of the structure corresponding to the rigid and pinned behaviour of horizontal inter-connections. The figures indicate that turning the behaviour of horizontal inter-connections from rigid to pinned behaviour has no consequence on the drift of the structure. A similar response is observed for both behaviour of the inter-connection and this suggests that the horizontal inter-connection does not require a classification system in the serviceability limit state. This is mainly due to the fact that both modular units have a same lateral stiffness and are subjected to a concentrated load with a similar amplitude, leading to obtain a same displacement. Therefore, to save computation time, one can safely assign rigid behaviour to horizontal inter-connections in the design process of modular structures.

### 5.2.2. Classification of vertical inter-connections

The vertically stacked modules depicted in Fig. 6 (b) are assumed to

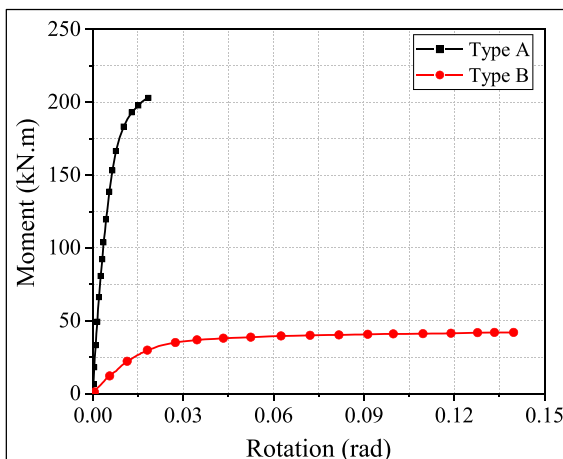


Fig. 29. Moment-rotation curves of selected inter-connections from [31,32].

scrutinise the influence of the rotational stiffness of vertical inter-connections on the drift of the second storey in the serviceability limit state. First, a displacement analysis is performed for the case of rigid intra-connection ( $\rho \approx 0.0$ ) to investigate the effect of the behaviour of vertical inter-connections. Fig. 23 (a) and 22 (b) show the drift of the second storey corresponding to rigid and pinned behaviour of the vertical inter-connections.

The figures indicate that while the drift varies between 2.0 and 4.5 for rigid vertical inter-connections, change in the behaviour of vertical inter-connections leads to an increase in the response of the structure. The drift of the second storey changes from 2.0 to 5.5 in pinned behaviour of vertical inter-connections. The comparison of rigid and pinned behaviour of vertical inter-connections, shown in Fig. 23 (c), indicates that when the relative bending stiffness ratios lie within the grey zone, the influence of rotational stiffness of vertical inter-connections on the drift is less than 5%, and its effect can be ignored in the modelling of a structure. On the other hand, the  $\delta_D$  reaches 40% in some relative bending stiffness ratios, indicating that it is required to determine the boundary between rigid and semi-rigid zones. Second, the flexibility of intra-connections is increased to  $\rho$  of 0.01 to incorporate the effect of rigidity of intra-connections on the boundary values of the classification system. The drift of the second storey corresponding to rigid and pinned behaviour of vertical inter-connections are shown in Fig. 24 (a) and 23 (b), respectively. The figure indicates that the response of the structure varies between 2.0 and 4.5 when inter-connections have a rigid behaviour. On the other hand, a drift between 2.0 and 6.5 is observed when a pinned behaviour of inter-connections is employed in the structure. The comparison of the rigid and pinned behaviour, shown in Fig. 24 (c), illustrates that the  $\delta_D$  varies up to 40%. For the grey zone, where the stiffness of inter-connections affects the drift less than 5%, the rigidity of inter-connections can be ignored in the modelling. For the rest, the boundary values corresponding to the rigid/semi-rigid zones need to be determined. Comparing the relative bending stiffness of inter-connections with the boundary zone can help structural engineers to understand how the stiffness of inter-connections needs to be considered in the modelling of a sway modular frame.

Fig. 25 (a) and 24 (b) show the drift of the considered vertically stacked modular building in rigid and pinned behaviour when the relative bending stiffness ratio of intra-connection lies within the semi-rigid zone, i.e.,  $\rho = 0.05$ , respectively. The obtained responses show that the decrease of the rigidity of intra-connections leads to a slight increase in the drift of the second storey. The response varies from 2.0 to 4.5 when the inter-connections have a rigid behaviour. The former corresponds to higher relative bending stiffness ratios of joints, and the latter corresponds to lower relative bending stiffness ratios of joints. On the other hand, the drift of the structure varies from 2.1 to 6.0 in the case of pinned behaviour of vertical inter-connections. The  $\delta_D$ , shown in Fig. 25 (c), illustrates the shrinkage of the grey zone compared to the rigid behaviour of intra-connections. Furthermore, it is seen that this parameter reaches up to 40% in some relative bending stiffness ratios of joints. For those cases that fall within the grey zone, the stiffness of vertical inter-connections has no effect on the drift of the structure; hence, it can be modelled by a rigid element. On the contrary, for the rest, the boundary values corresponding to rigid/semi-rigid behaviour should be clarified. Moreover, the  $\delta_D$  is far less than 75% which is set to determine the boundary values of semi-rigid/nominally-pinned behaviour. This shows that the vertical inter-connection may have either rigid or semi-rigid behaviour.

Finally, the flexibility of the intra-connection is increased to  $\rho = 0.1$  to determine the effect of a semi-rigid behaviour of intra-connections on the boundary values corresponding to rigid/semi-rigid and semi-rigid/nominally-pinned zones, respectively. The displacement analysis of rigid and pinned behaviour of vertical inter-connections are displayed in Fig. 26 (a) and 25 (b). The comparison of these two behaviours, shown in Fig. 26 (c), specifies that the  $\delta_D$  varies from less than 5% (grey zone) to

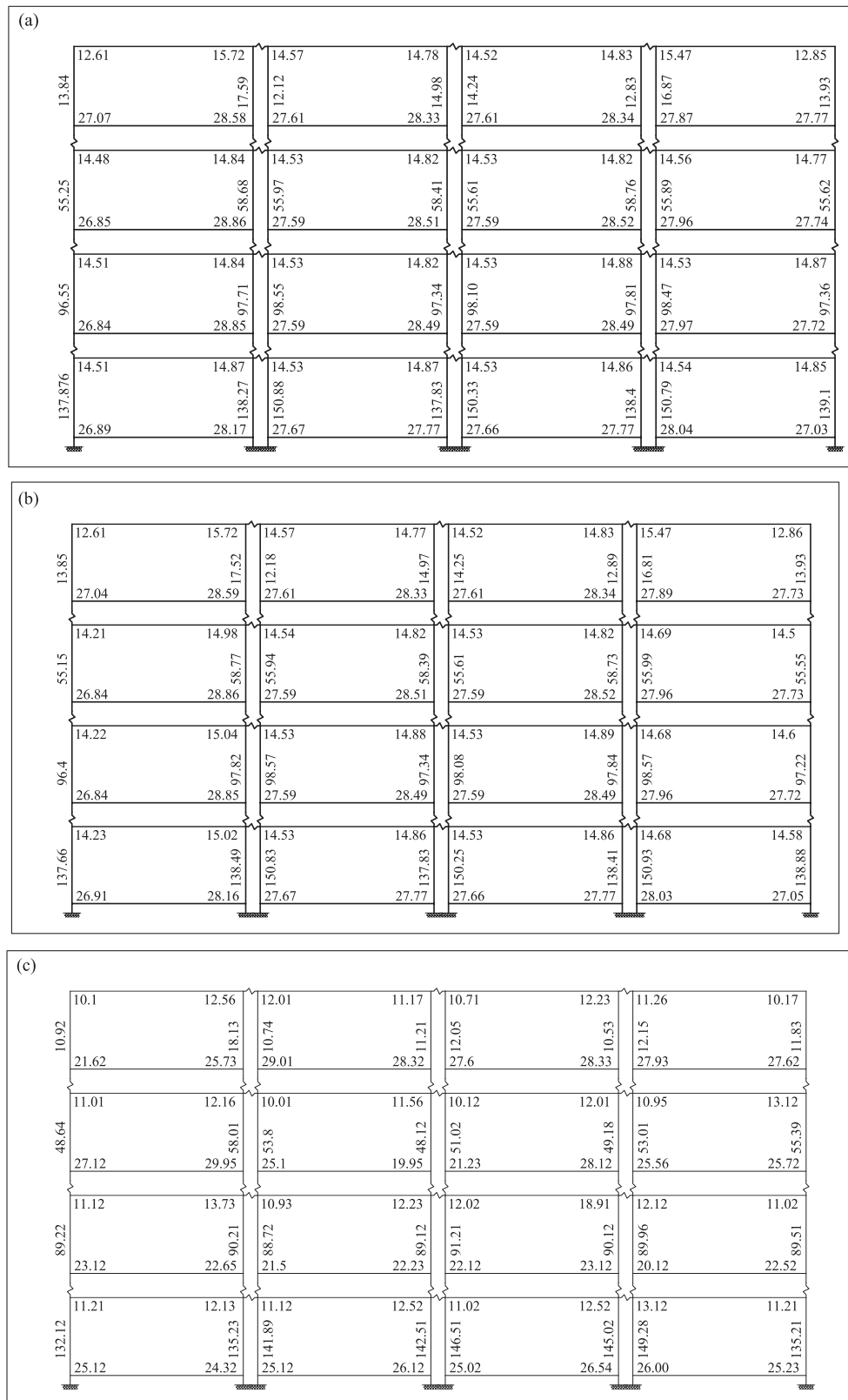


**Fig. 30.** The internal forces in the considered case study sway modular frame with (a) rigid inter-connections, (b) type "A" vertical inter-connections, (c) type "B" vertical inter-connections.

40% depending on the relative bending stiffness ratios at ceiling and floor levels. The grey zone indicates that the rotational stiffness of inter-connections does not affect the drift of the structure in the serviceability limit state, and the structure can be modelled without the need for

considering into account the stiffness of the inter-connections. For the rest, a classification system is required to determine whether a connection behaves rigidly or semi-rigidly. The figure also illustrates that the maximum obtained  $\delta_D$  is far less than 75%. Therefore, the

boundary value corresponding to semi-rigid/nominally-pinned behaviour is not required.

Using the contour charts above, it is vital to characterize the boundary values corresponding to the rigid/semi-rigid zones. To that end, a series of displacement analyses have been performed to determine the relative bending stiffness ratios of vertical inter-connections corresponding to a 5% increase in the drift of the second storey. The results are plotted in Fig. 27 (a) to (d). The charts suggest that the boundary values between rigid and semi-rigid zones vary from 0.5 to 9.0 in all rigid and semi-rigid intra-connections, depending on the relative bending stiffness ratios of joints at floor and ceiling levels. For example, as per highlighted for  $G_E = G_M = 0.489$  and  $G_I = G_Q = 0.182$ , the relative bending stiffness ratio of inter-connections must be at least 3.3 to be classified as a rigid inter-connection. In this case, the variation in the lateral drift/displacement of a joint in the structure is less than 5% corresponding to rigid behaviour. Therefore, the joint in the sway corner-supported modular frame can be modelled as a continuous joint. Otherwise, the rigidity of the connection must be taken into account during the modelling and analysing of a structure, and its influence on the dynamic characteristics of the structure should be considered. The verification and guideline on how to use the charts are provided through an example in the next section.

## 6. Case study

### 6.1. Preliminary design

The reliability of the proposed classification system for the inter-connections in sway corner-supported modular frames is investigated through the use of various rotational stiffness of inter-connections which are available in the literature [31,32] and study their influence on the internal forces of beams and columns of a 2D sway modular frame. The elevation view of the assumed 2D frame is illustrated in Fig. 28. The structure will be used to control the rigidity of the inter-connections according to the combined buckling and displacement criterion at the ultimate limit state, described by Eq. (3). The horizontal and vertical inter-connections are depicted by springs in the figure. The modules are connected in the horizontal direction at floor and ceiling levels. The vertical connectivity is provided by connecting the top part of the columns to the base of the next level column. Since the intra-connections are assumed to be moment connections, they are modelled by rotational springs having a large stiffness. The considered frame for assessing the reliability of the developed classification system is a perimeter frame of a four-storey building. (See Fig. 29.)

The selected building is a residential corner-supported sway modular

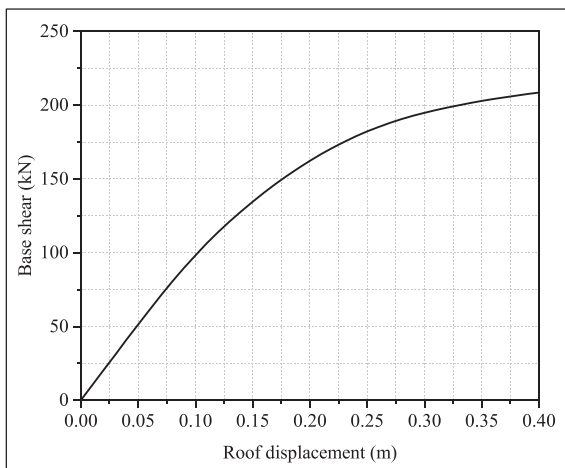


Fig. 31. Pushover result of the case study building assuming rigid behaviour for vertical and horizontal inter-connections.

structure composed of four modules in the Y direction and five modules in the X direction. Each module comes with a floor and ceiling, in which the floor is composed of the floor beams, joists, floor metal deck, and concrete topping. Similarly, the ceiling is composed of ceiling beams and joists. Each module unit has a dimension of  $6.1\text{ m} \times 3.6\text{ m} \times 3.1\text{ m}$  corresponding to width, length, and height, respectively. It is assumed that each module has a distance of 0.2 m to the adjacent modules in both X and Z directions, allowing the mechanical services to run between modules. The total in-plane dimension of the module in the X direction is 25.0 m, and the total height of the frame is 11.8 m in height. The central module is employed as a corridor to give access to the units. The selected frame is designed according to the assumption that it is constructed in the east part of the United States, which is a relatively low seismic region. The American Institute Steel Construction (AISC 360-16) [33] is used for the preliminary design of the steel building. The Minimum Design Loads and Associated Criteria for Buildings and Other Structures (ASCE 7-16) [34] is used for the calculation of the gravity as well as lateral loads due to the earthquake and wind actions [35,36]. The seismic parameters of the  $S_s$  and  $S_1$  are selected based on the ASCE 7-16, which are 0.275 and 0.58, respectively. The structure is built on a site classified as site class D based on the soil classification of ASCE 7-16. To design the structure against the earthquake actions, the equivalent lateral force (ELF) procedure is chosen. The response modification factor ( $R$  factor), deflection amplification factor ( $C_d$ ), and overstrength factor ( $\Omega_0$ ) corresponding to the intermediate moment frame suggested by ASCE 7-16 are selected to determine the earthquake actions. These factors are selected due to the fact that no research has been conducted to obtain their seismic performance factors. The live load equals 1.92 kPa, 0.96 kPa, and 4 kPa is assumed for the floor ( $LL_f$ ), ceiling ( $LL_c$ ), and corridor, respectively. The simplified model of the structure is developed in the FEM software SAP2000, in which the inter-connections are modelled by link elements. The selected sections are, therefore, HSS 5x5x3/8 for columns, HSS 6x4x1/4 for floor beam, and HSS 4x4x1/4 for ceiling beam elements.

In order to check the validity of the proposed classification systems, two types of inter-connections are selected from [31,32]. The first connection, namely type "A" connection, has been studied experimentally, theoretically and numerically to derive its moment-rotation response [31]. The inter-connection is an end plate connection which can provide the connectivity in both horizontal and vertical directions. The second considered inter-connection, suggested by Chen et al. [32], is the corner fitting connection. This inter-connection which can provide the vertical connectivity between modules is named type "B" in this paper. Chen et al. conducted experimental study and numerical simulations to investigate the failure modes and moment-rotation response of the considered connection. Fig. 28 compares the moment-rotation responses of selected inter-connections replotted from [28, 29]. The rotational stiffness of both inter-connections can be obtained from the results of cyclic and monotonic tests provided by [28,29]. The rotational stiffness of the first inter-connection is 16,783.32 kN.m/rad and that of the second inter-connection is 2391.49 kN.m/rad.

### 6.2. Validation of the proposed classification system

The internal forces of the elements, including moments at the end of the beams and axial load in the columns, are considered as desired responses under the unfactored loads. Furthermore, the effective length factor of columns in the structure is checked for the classification of inter-connections. To obtain the effective length factor and check the rigidity of the inter-connections, the relative bending stiffness ratios of horizontal and vertical inter-connections ( $SR_H$  and  $SR_V$ ), as well as the relative bending stiffness ratios of joints ( $G'$  ratios) need to be determined. The relative bending stiffness ratios of the floor and ceiling beams to column are 0.489 and 0.182, respectively. The relative bending stiffness ratio of inter-connections to the column, calculated through Eq. (10), are 24.77 and 3.9, respectively. Due to the lack of sufficient

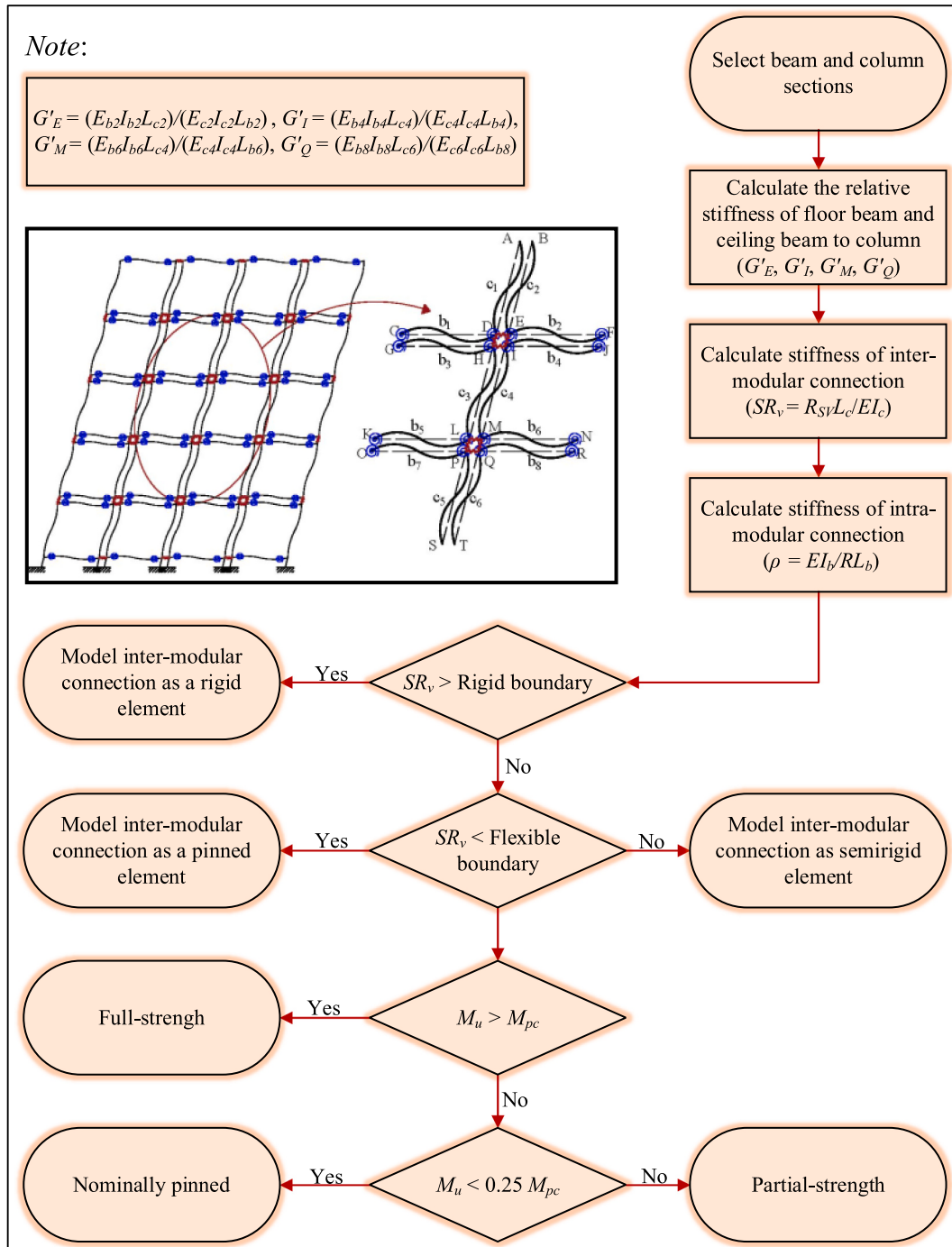


Fig. 32. Flowchart of recommendation of design of a modular structure.

information for horizontal inter-connections, it is assumed that the same connections are used for horizontal inter-connections. The results of the effective length factor for different stiffness of horizontal inter-connections indicated that its stiffness has no effect on the effective length factor of a column, and it remains constant for both pinned and rigid behaviour of inter-connection. Therefore, both connections are classified as rigid horizontal inter-connections. On the other hand, it is seen that the behaviour of vertical inter-connections affects the buckling capacity and drift of the structure. With reference to Fig. 13 (c), turning the behaviour of a rigid vertical inter-connection to pinned inter-

connection can decrease the buckling capacity by almost 20% for the considered  $G'$  ratios. This indicates that the relative bending stiffness ratio of the employed vertical inter-connections should be controlled with the established classification charts, shown in Fig. 17 (a), to determine the connections fit into the rigid or semi-rigid zones. According to the figure, for the considered modular frame, it is seen that the relative bending stiffness ratio of type "A" inter-connections is higher than of the boundary value corresponding to the rigid/semi-rigid zones. On the other hand, the relative bending stiffness ratio of type "B" inter-connection is less than the boundary condition corresponding to

the relative bending stiffness ratio of considered joint. Therefore, the type "A" inter-connection is considered as a rigid inter-connection and the type "B" inter-connection is considered as a semi-rigid inter-connection in the ultimate limit state.

To demonstrate the effect of the stiffness of inter-connections on the internal force distribution, the analysis results of the considered 2D modular frame employing the rigid vertical inter-connections are compared with those of the type "A" and "B" as vertical inter-connections, which are shown in Fig. 30. The results indicate that the type "

A" inter-connection behaves as a rigid connection due to the fact that the internal forces do not vary more than 5%. On the other hand, it is seen that the moment at the end of some elements varies more than 5%, when the type "B" inter-connection is employed. The results obtained through the analysis of the 2D frame using horizontal inter-connection illustrate that the internal forces vary less than 5%. Hence, they can be modelled by rigid elements.

The ultimate moment resistance of connections is compared with the design plastic moment resistance of the inter-connections' adjacent column to investigate their classification system based on the strength properties. The design plastic moment resistance of the column 5x5x3/8 is 78.165 kN.m. Comparing the ultimate moment resistance of the connections with the design moment resistance of the column shows that type "A" inter-connection is categorized as full-strength. On the other hand, the type "B" connection is classified as partial-strength.

### 6.3. Classification of stiffness based on the combined buckling and displacement at ultimate limit state

In order to evaluate the rigidity of the inter-connections for combined buckling and displacement at the ultimate limit state, the validity of Eq. (3) is verified for both inter-connections, which are used as horizontal and vertical inter-connections in the case study building. The modelling and analysing of the structure in the ultimate limit state are performed by OpenSees software. The Steel02 material and fiber sections are assigned to the beam and column elements to consider the material nonlinearity of steel elements. To determine the displacement of the roof of the structure at the ultimate limit state, the gravity load is assigned to the beam elements, and then the lateral load, in the form of the triangle pattern, is monotonically increased. Once the end moment in one of the elements of the structure reaches to its design plastic moment, the analysis will terminate, and the displacement of the roof is monitored. Fig. 31 shows the base shear vs. roof displacement of the structure obtained from pushover analysis. The ultimate displacement of the structure for the case of rigid inter-connections is obtained as 0.115 m. The pushover analysis illustrates that the displacement of the structure at the ultimate limit states is the same as that of the rigid inter-connections, when both type A and B connections are used as horizontal inter-connections. On the other hand, the results obtained from the pushover analysis indicate that the displacement of the structure varies 0.3% and 1.5% when the type "A" and "B" connections are used as vertical inter-connections, respectively. Substituting the effective length factor and displacement at the ultimate limit states for both inter-connections into Eq. (3) indicates that the type "A" inter-connection behaves as a rigid inter-connection for the case study building. On the other hand, the type "B" inter-connection behaves as a semi-rigid inter-connection.

## 7. Design recommendations

This section provides a procedure for modelling, analysing, and designing of horizontal and vertical inter-connections in a sway corner-supported modular frame. The procedure for the accurate design of inter-connections is briefly explained in a flowchart form shown in Fig. 32. In order to classify the inter-connections for use in the design of a modular frame, the mechanical properties of both inter- and intra-

connections are required, which can be obtained through conducting experimental tests or advanced finite element simulations. Having the mechanical properties of the intra-connections, its stiffness can be compared with the available classification system for beam-to-column connections provided by Eurocode 3 to control the rigidity of the intra-connections. In the preliminary design of the sway modular building, all inter-connections can be assumed to have a rigid stiffness to select appropriate sections for columns and beams. The next step is to calculate the relative bending stiffness ratios at the floor and ceiling levels. Having in mind that the rotational stiffness of the horizontal inter-connection does not influence the effective length factor and drift of the structure, it can be considered as a rigid element in the mathematical model of the structure. On the other hand, the relative bending stiffness ratio of the vertical inter-connections may be compared with the provided boundary conditions for rigid/semi-rigid as well as semi-rigid/nominally-pinned zones to determine the rigidity of the inter-connections and judge how it should be modelled in the numerical modelling of the structure. Finally, the ultimate moment capacity of both horizontal and vertical inter-connections can be compared with the design plastic moment of their adjacent columns to fit the inter-connection in one of the available classification systems based on the strength properties.

## 8. Conclusion

This study presents a classification system for horizontal and vertical inter-connections in sway corner-supported modular frames. The classification system is established for both strength and stiffness properties of inter-connections. The validity of the established classification system is demonstrated through a numerical example where the distribution of forces in elements is compared for two different inter-connections. Based on the numerical results and validation against numerical example, the following conclusion have been drawn:

- The effective length factor of a column in a horizontally connected modular structure with rigid behaviour of intra-connection varies between 1.4 and 2.5 for both rigid and pinned behaviour of horizontal inter-connections. This indicated that, the rotational stiffness of horizontal inter-connections has no effect on the buckling capacity of columns. Therefore, its behaviour has no effect on the buckling capacity of columns.
- The rotational stiffness of vertical inter-connection, can change the buckling capacity of columns from less than 5% up to more than 75%, depending on the stiffness of intra-connections.
- The minimum rigidity of relative bending stiffness ratio of vertical inter-connection to classify the connection as a rigid inter-connection, is a function of stiffness of joint and intra-connection and varies from 0.5 to 15, when the intra-connections have a semi-rigid behaviour ( $\rho = 0.1$ ).
- The rotational stiffness of horizontal inter-connections has no effect on the drift of a horizontally connected modular structure. Hence, the rotational stiffness of horizontal inter-connections can be modelled by a rigid behaviour.
- The rotational stiffness of vertical inter-connections can influence the drift of a vertically modular structure. Compared to the rigid behaviour of vertical inter-connections, the use of pinned behaviour of vertical inter-connections can increase the drift of a vertically connected modular structure up to 40% for all behaviours of intra-connections.
- The obtained responses from drift analysis of a vertically stacked modular structure, indicate that the boundary values of rigid/semi-rigid zones of vertical inter-connections vary from 0.5 to 9 for all behaviour of intra-connections, depending on the relative bending stiffness ratios of joints.

## The following symbols are used in paper

$K_R$	K-factor of column in a portal frame with rigid connections	$S_h$	Horizontal inter-connection
$K_{SR}$	K-factor of column in a portal frame with semi-rigid connections	$S_v$	Vertical inter-connection
$K_p$	K-factor of column in a portal frame with pinned connections	$E$	Modulus of elasticity of elements
$\Delta_R$	Drift of a frame at serviceability limit state with rigid connections	$I_b$	Moment of inertia of beam
$\Delta_{SR}$	Drift of a frame at serviceability limit state with semi-rigid connections	$I_c$	Moment of inertia of column
$\Delta_P$	Drift of a frame at serviceability limit state with pinned connections	$L_b$	Beam length
$\Delta_{uR}$	Drift of a frame at ultimate limit state with rigid connections	$L_c$	Column length
$\Delta_{uSR}$	Drift of a frame at ultimate limit state with semi-rigid connections	$G_i$	Relative bending stiffness ratio of element
$M_u$	Ultimate moment of inter-connection	$SR_{iH}$	Relative bending stiffness ratio of horizontal inter-connection
$M_{pc}$	Plastic moment of column	$SR_{iV}$	Relative bending stiffness ratio of vertical inter-connection
$P_{cr}$	Critical buckling load	$\alpha_{bf}$	Flexibility coefficient

## Declaration of Competing Interest

The authors declared no potential conflicts of interest with respect to the research, authorship, and/or publication of this article.

## Data availability

Data will be made available on request.

## Acknowledgement

The authors acknowledge the support of Australian Research Council (ARC) grant DE190100113 in this research project and writing of this paper.

## References

- [1] P. Sharafi, et al., Identification of factors and decision analysis of the level of modularization in building construction, *J. Archit. Eng.* 24 (2) (2018) 04018010.
- [2] P. Sharafi, et al., Interlocking system for enhancing the integrity of multi-storey modular buildings, *Autom. Constr.* 85 (2018) 263–272.
- [3] A.W. Lacey, et al., Effect of inter-module connection stiffness on structural response of a modular steel building subjected to wind and earthquake load, *Eng. Struct.* 213 (2020), 110628.
- [4] M. Alembagheri, et al., Anti-collapse resistance mechanisms in corner-supported modular steel buildings, *J. Constr. Steel Res.* 170 (2020), 106083.
- [5] M. Alembagheri, et al., Collapse capacity of modular steel buildings subject to module loss scenarios: the role of inter-module connections, *Eng. Struct.* 210 (2020), 110373.
- [6] M. Farajian, P. Sharafi, K. Kildashti, The influence of inter-module connections on the effective length of columns in multi-story modular steel frames, *J. Constr. Steel Res.* 177 (2021), 106450.
- [7] M. Alembagheri, et al., Natural dynamic characteristics of volumetric steel modules with gypsum sheathed LSF walls: Experimental study, in: *Structures*, Elsevier, 2021.
- [8] P. Sharafi, et al., Automated spatial design of multi-story modular buildings using a unified matrix method, *Autom. Constr.* 82 (2017) 31–42.
- [9] E.-F. Deng, et al., Seismic behavior and design of cruciform bolted module-to-module connection with various reinforcing details, *Thin-Walled Struct.* 133 (2018) 106–119.
- [10] X.-M. Dai, et al., Experimental study on seismic behavior of a novel plug-in self-lock joint for modular steel construction, *Eng. Struct.* 181 (2019) 143–164.
- [11] CEN, Eurocode 3: Design of Steel Structures—Part 1–8: Design of Joints, European Committee for Standardization, Brussels, 2005.
- [12] M. Ivanyi, Semi-Rigid Joints in Structural Steelwork, 2000.
- [13] Y. Wang, L. Xue, Experimental study of moment-rotation characteristics of reverse channel connections to tubular columns, *J. Constr. Steel Res.* 85 (2013) 92–104.
- [14] M.H. Asl, B. Farivar, S. Momenzadeh, Investigation of the rigidity of welded shear tab connections, *Eng. Struct.* 179 (2019) 353–366.
- [15] I. Faridmehr, M.M. Tahir, T. Lahmer, Classification system for semi-rigid beam-to-column connections, *Latin Am. J. Solids Struct.* 13 (2016) 2152–2175.
- [16] I. Birkeland, A. Aalberg, S. Kvam, Classification boundaries for stiffness of beam-to-column joints and column bases, in: Proceedings of Nordic Steel Construction Conference, 2012.
- [17] R. Bjørhovde, A. Colson, J. Brozzetti, Classification system for beam-to-column connections, *J. Struct. Eng.* 116 (11) (1990) 3059–3076.
- [18] N. Kishi, W.-F. Chen, Data base of steel beam-to-column connections, in: Structural Engineering Area, School of Civil Engineering, Purdue University, 1986.
- [19] R. Hasan, et al., Evaluation of rigidity of extended end-plate connections, *J. Struct. Eng.* 123 (12) (1997) 1595–1602.
- [20] R. Hasan, N. Kishi, W.-F. Chen, A new nonlinear connection classification system, *J. Constr. Steel Res.* 47 (1–2) (1998) 119–140.
- [21] Y. Goto, S. Miyashita, Validity of classification systems of semirigid connections, *Eng. Struct.* 17 (8) (1995) 544–553.
- [22] Y. Goto, S. Miyashita, Classification system for rigid and semirigid connections, *J. Struct. Eng.* 124 (7) (1998) 750–757.
- [23] F.C. Gomes, P. Providência, R. Costa, Classification of reinforced concrete beam-to-column joints, in: CoRAN 2011—international conference on recent advances in nonlinear models—structural concrete applications, Coimbra, 2011.
- [24] D. Nethercot, T. Li, B. Ahmed, Unified classification system for beam-to-column connections, *J. Constr. Steel Res.* 45 (1) (1998) 39–65.
- [25] F. Fan, et al., A new classification system for the joints used in lattice shells, *Thin-Walled Struct.* 49 (12) (2011) 1544–1553.
- [26] W. Wang, Y. Chen, Modelling and classification of tubular joint rigidity and its effect on the global response of CHS lattice girders, *Struct. Eng. Mech. Int.* 21 (6) (2005) 677–698.
- [27] F. Bijlaard, C. Steenhuis, Prediction of the influence of connection behaviour on the strength, deformations and stability of frames, by classification of connections, in: Bjørhovde, et al. (Eds.), *Connections in Steel Structures II*, American Institute of Steel Construction, Chicago, 1992.
- [28] F.C. Gomes, The EC3 classification of joints and alternative proposals, *Eurosteel Coimbra* (2002) 987–996.
- [29] N. Kishi, et al., Effective length factor of columns in flexibly jointed and braced frames, *J. Constr. Steel Res.* 47 (1–2) (1998) 93–118.
- [30] S. Mazzoni, et al., OpenSees Command Language Manual vol. 264, Pacific Earthquake Engineering Research (PEER) Center, 2006.
- [31] X. Liu, et al., Bending-shear performance of column-to-column bolted-flange connections in prefabricated multi-high-rise steel structures, *J. Constr. Steel Res.* 145 (2018) 28–48.
- [32] Z. Chen, et al., Rotational stiffness of inter-module connection in mid-rise modular steel buildings, *Eng. Struct.* 196 (2019), 109273.
- [33] ANSI/AISC, AISC 360–16, Specification for Structural Steel Buildings, American Institute of Steel Construction, Chicago, IL, 2016.
- [34] ASCE/SEI 7, Minimum Design Loads and Associated Criteria for Buildings and other Structures, American Society of Civil Engineering & Structural Engineering Institute: Reston, Virginia, 2016.
- [35] N. Usefi, P. Sharafi, H. Ronagh, Numerical models for lateral behaviour analysis of cold-formed steel framed walls: state of the art, evaluation and challenges, *Thin-Walled Struct.* 138 (2019) 252–285.
- [36] P. Sharafi, et al., Lateral force resisting systems in lightweight steel frames: recent research advances, *Thin-Walled Struct.* 130 (2018) 231–253.